

POST-FIRE EFFECTS ON HYDROLOGICAL AND ERODIBILITY FACTORS IN A SIMULATED BURN AND RAINFALL EXPERIMENT

by

Annelies Voogt

MSc Thesis



July, 2010

POST-FIRE EFFECTS ON HYDROLOGICAL AND ERODIBILITY FACTORS IN A SIMULATED BURN AND
RAINFALL EXPERIMENT

Annelies Voogt

Thesis submitted for partial fulfillment of the requirements of the
MSc degree in International Land and Water Management at
Wageningen University, the Netherlands

Study program
MSc International Land and Water Management (MIL)

Student registration number
850806 903 050

Thesis Land Degradation and Development
LDD-80306

Supervisors:

Dr. Saskia Keesstra (Land Degradation and Development Group, Wageningen University)
Dr. Lea Wittenberg (Department of Geography and Natural Environment, Haifa University, Israel)
Dr. Eli Argaman (Soil Erosion Research Station, Ruppin, Israel)

Examinators:

Dr. Saskia Keesstra
Dr. Lea Wittenberg

Preface and acknowledgments

This report is the product of my thesis research project which is part of the MSc program International Land and Water management at Wageningen University and Research Centre (WUR). The research has been carried out at the forest of Biriya, province Upper Galilee and the Soil Erosion Research Centre (SERS) in Israel. The field work is connected to the larger research project of dr. Wittenberg and dr. Malkinson in fire-affected forests in northern Israel, funded by the Jewish National Fund. The objectives of this project were to assess the impacts on forest fires on the sediment composition of the drainage system discharging in the Sea of Galilee, a main source of fresh water supply for Israel.

I want to thank the whole staff of the Department of Geography and Environment at Haifa University for the wonderful time, but most of all Lea Wittenberg for all the guidance she gave me in the field and laboratory. It turned out that I could learn and experience a lot from both locations. I was warmly welcomed by colleagues in Haifa and at the Soil Erosion Research Station, especially during lunchtime and coffee breaks. I remember having many small talks with Arnon about social geographical issues in Israel.

Na'ama, I want to thank for the support in the research process and for showing me around in the beautiful Carmel Park and its surroundings. With you doing research there, the Park will become cleaner and more flourishing than ever!

Dan and Eldan were perfect colleagues as they both preferred the field above computer work, resulting in many trips to the forest and Jordan river, which were interesting and very enjoyable. Also, I want to

With the shift of the research to laboratory simulation I happened to be able to stay for a considerable time at the slightly male-dominated and beautifully situated Soil Erosion Research Station. I want to thank Eli for the supervision on the experimental part and his ideas and suggestions concerning the entire research. You supported me a lot in staying focused in handling the loads of data. The technicians Froyke and Moshik gave unconditional help during the experiment. Also I thank Ruti for her great hospitality as I could stay at her home for more than two weeks. And for the delicious lunches at the station every day!

Back home in the Netherlands my supervisor Saskia Keesstra was of great support during the process of analysis and writing. She was also the first facilitator of the contacts with Israel and provided me the opportunity to do my thesis research there.

However longer than planned, the period back home spend with several MSc- and PhD-students in one office was academically valuable and enjoyable.

My roommates, friends and family in the Netherlands and Israel were irreplaceable in their support during this last stage of my master study. I thank God for them and for his world that we explore!

Todah rabah!

Annelies Voogt
Wageningen, July 2010

Abstract

Mediterranean forests are frequently subject to wildfires, inducing risks of runoff and loss of nutrient-rich topsoil. A recent fire in Biriya forest, northern Israel, and related post-fire observations set the stage for laboratory fire (manual) and rainfall (nozzle-type) simulation experiments to evaluate short-term effects of fire on soil hydrological and erodibility parameters by investigating (i) soil water repellency (WR) levels and distribution, (ii) surface cover features, and (iii) sat. hydraulic conductivity (K_{sat}), electrical conductivity and values of infiltration, runoff and erosion responses to simulated rain on control (bare and needle covered) and burned (with and without ash cover) samples. To link the laboratory observations to the field situation, WR, K_{sat} and surface cover measurements were executed in the forest.

Field data showed strong surface WR levels throughout the rainy season, indicating the high severity of the fire. The fire-induced surface WR in the lab, tested by grid-wise Water Drop Penetration (WDPT) tests, was moderate but decreased for all treatments after rain. The responses to rain (33 mm h^{-1}) differed for the two simulation runs. The rates of drainage and runoff of the burned samples showed in the first run values in between the values of cover (low runoff, high infiltration) and bare (high runoff, low infiltration). The drainage in the ash-covered samples was twice as high as in the samples where the ash was removed. In the second run both samples showed a similar response compared to bare conditions. After the first run most ash and organic material was washed off and K_{sat} was low, indicating crust formation. If upscaled, sediment yields reached in run 1 and 2 resp. 0.2 and $0.8 \text{ t ha}^{-1} \text{ h}^{-1}$. After the first run the EC values showed a significant drop, which represents the infiltration of the cation-binding organic matter, as this is not present for the bare samples. When field and laboratory observations are combined it can be stated that apart from soil crusting, WR and protection by ash are factors to consider in erosion susceptibility of a burned forest soil.

Key words: soil water repellency, fire simulation, rainfall simulation, soil erosion, sediment loss, ash cover, Mediterranean wildfires, vegetation recovery

Table of contents

1. Introduction.....	1
1.1 MEDITERRANEAN WILDFIRES	1
1.2 SOIL WATER REPELLENCY	2
1.3 FIRE-INDUCED EROSION	3
1.4 SIMULATION OF FIRE AND RAIN.....	4
2. Objectives and research questions	5
3. Study area	6
4. Methodology.....	8
4.1 FIELD EXPERIMENTS	8
5.1.1 Surface cover changes	8
4.1.2 Water repellency.....	8
4.1.3 Saturated hydraulic conductivity	9
4.2 LABORATORY SIMULATIONS	10
4.2.1 Characteristics of soil and treatments	10
4.2.2 Fire simulation	11
4.2.3 Water repellency.....	13
4.2.4 Rainfall simulation and analysis	13
4.2.5 Saturated hydraulic conductivity	14
4.2.6 Hyperspectral sampling	15
4.2.7 Sections of soil sample volumes	16
4.3 ANALYSIS	16
5. Results.....	17
5.1 FIELD EXPERIMENTS	17
5.1.1 Surface cover changes	17
5.1.2 Water repellency.....	17
5.1.3 Saturated hydraulic conductivity	18
5.2 LABORATORY SIMULATIONS	18
5.2.1 Soil characteristics	18
5.2.2 Fire simulation characteristics	19
5.2.3 Water repellency.....	19
5.2.4 Hydrologic responses rainfall simulation	20
5.2.5 Saturated hydraulic conductivity	26
5.2.6 Hyperspectral signatures	28
5.2.7 Sections of soil sample volumes	28
6. Discussion.....	30
6.1 EROSION PARAMETERS	30
6.1.1 Vegetation.....	30
6.1.2 Soil physics and hydrology	31
6.1.3 Ash cover.....	32
6.1.4 Water repellency.....	33
6.2 EXPERIMENTAL SET-UP	35
7. Conclusion	37
7.1 IMPLICATIONS	38
7.2 FURTHER RESEARCH	38
8. References	39

List of Annexes

- I. Classified feature maps field
- II. Map overlay of WR grid and picture
- III. Map overlay of Preferential flow and photo
- IV. Classified feature maps laboratory
- V. Close-up photos of soil samples

List of Figures

Figure 1 Part of the burned Peér'am catchment, July 2009	1
Figure 2 Schematic representation of an amphiphilic organic molecule and changes in orientation of such molecules on a mineral surface in contact with water (taken from Doerr <i>et al.</i> , 2000)	3
Figure 3 Maps of study area field experiments	6
Figure 4 Ash layer on mineral soil and estimating depth of uprooted tree hole	7
Figure 5 Burned hillslope 8th of Nov, 2009 and 17th of Jan, 2010	7
Figure 6 Schematic drawing of locations WDPT test in circles of 0.5 and 1 m around tree trunk	8
Figure 7 Hydrophobicity just below the ash layer in plot 4	8
Figure 8 Mini Disk Infiltrometer diagram (Decagon Devices) and measurement in the field	9
Figure 9 Tray preparation	10
Figure 10 Procedure of fire simulation	11
Figure 11 Simplified scheme of the chain of post-fire erosion processes during a rainy season	12
Figure 12 Grid for WDT test; shaded area is not measured	13
Figure 13 Side-view of grid with applied drop	13
Figure 14 Working principle of rotadisk rainulator	14
Figure 15 High Intensity Contact Probe (ASD Inc.)	15
Figure 16 Subdivision of surface into 5 sections where each 3 spectral signatures are taken	15
Figure 17 Soil water repellency level and occurrence in burned field and control	17
Figure 18 Weight fraction of each aggregate class in the sampling soil	18
Figure 19 Drainage patterns (mm h^{-1}) during the first rainfall simulation run	22
Figure 20 Drainage pattern (mm h^{-1}) during the second rainfall simulation run	22
Figure 21 Runoff patterns (mm h^{-1}) during the first run	22
Figure 22 Runoff patterns (mm h^{-1}) during the second run	22
Figure 23 Sedigraphs of the first rainfall run for all burned and bare treatments	24
Figure 24 Sedigraphs of the second rainfall run for all burned and bare treatments	24
Figure 25 Patterns of EC of drainage water in 1 st and 2 nd rainfall run	24
Figure 26 Patterns of EC of runoff water in 1 st and 2 nd rainfall run	24
Figure 27 Spectral signatures of averaged point measurements on five sections of the surfaces of samples	27
Figure 28 Spectral signature curves of cover and +ash samples for 1.25-2.5 μm range at three moments during the rainfall series.	28
Figure 29 Close-up of crust of bare sample, with accumulated salts (white spots) at bottom.	29
Figure 30 Close-ups of cemented aggregates and organic material in lower horizon of a) +ash, b) –ash.	29
Figure 31 Mean runoff rate over time for the bare-soil, low-ash and high-ash treatments for granitic and micaceous soil (taken from Larsen <i>et al.</i> , 2009)	33

List of Tables

Table 1 Changes in aboveground vegetation and soil organic matter related to fire severity	2
Table 2 Classification Water Drop Penetration time test (adjusted to Tessler <i>et al.</i> , 2008)	8
Table 3 Characteristics of the experimental trays	11
Table 4 Timing of simulation and tests, in days after the burn	12
Table 5 Fraction of surface cover features field plots 1-5 at moments 4 and 6 months after the fire (%)	17
Table 6 Saturated hydraulic conductivity, soil moisture and penetration resistance of the study plots	18
Table 7 Frequency of water repellency levels for 2 WDPT tests (in # of grid cells)	19
Table 8 Runoff and erosion data of the rainfall simulation experiments	21
Table 9 Fraction cover features on burned treatments before 1 st and 2 nd rainfall run	25
Table 10 K_{sat} values (in mm h^{-1}) of first (MDI1) and second (MDI2) measurements	26

Abbreviations and acronyms

ASD	ASD Spectrometer
4/15 -ash	soil sample with aggregate size 4 or 15 which is burned and where the ash is removed before rainfall simulation
4/15 +ash	soil sample with aggregate size 4 or 15 which is burned and is placed undisturbed under the rainfall simulation
4/15 bare	control soil sample with aggregate size 4 or 15 without any soil cover
4/15 cover	control soil sample with aggregate size 4 or 15 and needle soil cover
K_{sat}	Saturated hydraulic conductivity
MDI	Mini Disk Infiltrometer
SERS	Soil Erosion Research Station
WDPT	Water Drop Penetration Time test
WR	water repellency

1. Introduction

1.1 MEDITERRANEAN WILDFIRES

The natural environment in the Mediterranean Basin ecosystems is vulnerable to wildfires, as it is situated in a landscape of long-lasting human impact, with low precipitation rates, no rain in the dry season and highly flammable vegetative types and forest floors. Since the 1970s the Mediterranean area subject to a wildfire has increased from 300 to 600 kha (FAO, 1998). In addition to this, climatic change may induce the amount of fires as a higher summer air temperature and less precipitation decrease the fuel humidity (Pausas and Vallejo, 1999). This poses a risk of increased erosion in the Mediterranean landscape.

The Biriya forests in the mountains of Galilee, northern Israel, have suffered from several wildfires in the recent years. During the summer of 2006 Israel-Hezbollah war the north of Israel was attacked by katyusha rockets, initiating fires in the conifer forests of the Navuraya catchment of Biriya forest (basin area 1.1 km²), damaging about 80 ha of tree area as well as the duff floor (Wittenberg and Malkinson, personal communication). In July 2009 another human-induced fire took place in a different part of the forest, in Peér'am catchment (Figure 1). The wildfire was intensive, with high temperatures, removing all needles and part of the branches of the pine trees in an area of 140 ha. In the parts of the highest fire severity complete trees were burned down, which were removed from the field.



Figure 1 Part of the burned Peér'am catchment, July 2009 (Source: Wittenberg, 2009)

In fire research fires are characterised in type, intensity and post-fire effects. According to Keeley (2009) fire intensity can be described as the physical combustion process of energy release from organic matter, expressed in energy per unit volume per velocity at which the energy is moving. To understand key processes as litter consumption and the development of repellent layers, knowledge is required of the duration of heating and maximum temperatures (Keeley, 2009).

Fire intensity can be translated to fire (or burn) severity, which comprises the impacts on vegetation and soil and is frequently used in literature to indicate the fire type (Robichaud, 2000); (Cerdà and Doerr, 2008; Ferreira *et al.*, 2008). It provides a description of the extent at which the fire affects the ecosystem. It should be taken into consideration that this conversion depends on factors such as pre-fire conditions and climate also (Keeley, 2009). Often the arrangement of fire severity levels is used according the index presented in Table 1 or metrics that share the same functionality.

The assessment of fire severity parameters for the impacts to soils include changes in soil structure and the development of water repellency (Keeley, 2009). The intensity and severity indices are central when they can predict responses in the ecosystem, like soil erosion and regeneration of vegetation. Ferreira *et al.* (2008) state that the degree of burn severity is directly related to post-fire erosion. In forest fire analysis associations with resprouting of undergrowth, forest recovery and plant alienation are key factors. And as loss of aboveground biomass exposes more soil surface, it is an important indicator of the potential for water runoff and erosion (Keeley, 2009). However, the link between fire severity and water repellency level is somewhat more vague, as it depends on depth, connectivity of water repellent layers and pre-fire conditions.

Table 1 Changes in aboveground vegetation and soil organic matter related to fire severity; taken from Keeley (2009) and Ryan and Noste (1985)

FIRE SEVERITY	DESCRIPTION
Unburned	Plant parts green and unaltered, no direct effect from heat
Scorched	Unburned but plants exhibit leaf loss from radiated heat
Light	Canopy trees with green needles although stems scorched Surface litter, mosses, and herbs charred or consumed Soil organic layer largely intact and charring limited to a few mm depth
Moderate – severe surface burn	Trees with some canopy cover killed, but needles not consumed All understorey plants charred or consumed Fine dead twigs on soil surface consumed and logs charred Pre-fire soil organic layer largely consumed
Deep burning – crown fire	Canopy trees killed and needles consumed Surface litter of all sizes and soil organic layer largely consumed White ash deposition and charred organic matter to several cm depth

1.2 SOIL WATER REPELLENCY

Soil water repellency is a natural phenomenon and is especially found in coarse-textured soils (Elliot *et al.*, 2001; Huffman *et al.*, 2001), although the agents can be found in any soil (Doerr *et al.*, 2000). When water comes in contact with this water repellent system, droplets will be formed. The spherical shape of the droplets which will form on an impermeable surface, in this case the soil, are due to the dipolar characteristics of the water molecules having a net attractive force to the interior when the attractive forces of the surface molecules is smaller (Doerr *et al.*, 2000). On water repellent soil layers this is the case, due to the low tension cause by the organic compounds which coat the soil particles (Figure 2). Normally a class of organic chemicals in the lower layers of the duff are hydrophobic and create as a result an almost water impermeable layer by coating the particles (Pyne *et al.*, 1996). These hydrophobic components originate from plants that produce it to protect leaves from desiccation and to repel insects or microbes. Also some fungi are reported to exudate hydrophobic products.

Fire induced WR

When residing long enough (5-20 min) and with temperatures (175 – 280 °C) high enough wildfires can cause a major change in the soil water repellency (Lewis *et al.*, 2008).

By the combustion process the organic matter in the litter layer volatilizes partly and its composition changes by the fire. Due to the pressure gradient the compounds, partly hydrophobic, are forced downward in the soil profile.

During a fire soil temperatures are highest on the soil surface and decrease with depth at a steep gradient, as soil is a bad conductor of heat. It was found that for a moderate fire (max. 427 °C) the temperature at 2.5 cm depth is 166 °C and for a light burn (max. 249 °C) only 88 °C (DeBano *et al.*, 1979). Therefore, the organic compounds moving down condense on a cooler soil layer, which is often not deeper than several centimeters below the soil surface (DeBano, 2000; Letey *et al.*, 2003). Compared to wet soils, the hydrophobic substances move farther downward in dry soil, if temperature gradients allow that. But also on soil surfaces water repellency may be formed, considering the soil surface temperatures to be high enough.

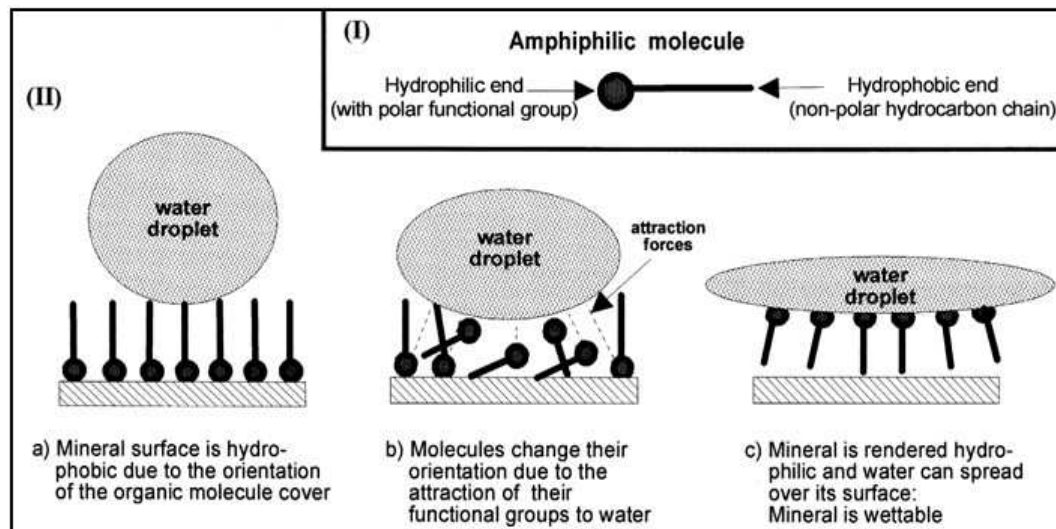


Figure 2 Schematic representation of (I) an amphiphilic organic molecule and (II/a-c) changes in orientation of such molecules on a mineral surface in contact with water (taken from (Doerr *et al.*, 2000))

The duration of soil water repellency varies between seconds to months after the fire, although in most fire-related cases it took several years to attain the pre-fire level (Doerr *et al.*, in press; Cerdà and Doerr, 2005). After a considerable time the layer diminishes, and brings the permeability of the soil back to pre-fire conditions (Certini, 2005), although this depends among other chemical, biological and physical processes on the soil moisture and the availability of macropores to agent the wetting process (Doerr *et al.*, in press). Organic matter content is positively correlated with soil water repellency, so complete combustion of the OM might diminish the retarding of infiltration (Mataix-Solera and Doerr, 2004).

It is found that a soil moisture threshold of 30% may be needed to change the state of the water repellent soil into wettable (Doerr *et al.*, in press). During the same fire it can however also be removed again, as DeBano (2000) adds that the hydrophobic components decompose at temperatures higher than 280 °C.

The effects of a fire on the soil water repellency depend on its temperature, the pre-fire existence and spatial variability of the hydrophobic components, the amount and type of litter consumed, the duration and amount of soil heating, and the amount of oxygen available during burning (Doerr *et al.*, in press). A scenario of increased, decreased or migrated water repellency layer might all be probable after a fire. In any case, connected soil layers with high water repellency hamper infiltration of rainfall water into deeper layers, increasing the risk of ponding water and slope wash.

1.3 FIRE-INDUCED EROSION

Besides generating high costs for society, forest fires destruct vegetation and affect the biological, chemical and physical properties of the soil.

The effect of wildfires on the soils and vegetation of Mediterranean ecosystems has received significant scientific attention (Certini, 2005), using field surveys (Inbar *et al.*, 1998; Neary *et al.*, 1999; Fox *et al.*, 2006; Lewis *et al.*, 2006; Úbeda and Mataix-Solera, 2008) as well as remote sensing techniques (Lentile *et al.*, 2006; Lewis *et al.*, 2008).

Depending on the intensity, fire alters physical and chemical properties of the soil and its effects can be subdivided in direct loss of nutrients (nitrogen) and effects due to changes in surface cover. The combustion removes (part of) the present canopy and undergrowth vegetation, exposing the mineral soil to water and wind. Next to that, it changes soil morphological and physical characteristics by breaking-down aggregates, cementing clay particles and inducing soil water repellency (e.g. DeBano, 2000). Sloping terrain which is burned in the summer and sparsely covered with vegetation is very susceptible for increased erosion of the soil, especially with the

characteristic Mediterranean conditions of intensive seasonal rains during the winter period. The fires in Biriya forest of 2006 combusted large parts of the nutrient-rich litter layer and topsoil and locally the soil was baked into a hard crust due to the breakdown of aggregates (Bodner, 2007). Runoff rates and sediment yields were therefore higher in the post-fire period, especially in the first rainy season after the fire. Malkinson and Wittenberg (2008) found values for runoff coefficients (ratio runoff/rainfall) to be >10% in the winter of 2006-2007, compared to values of 2% for areas covered with Mediterranean forest vegetation.

In general, post-fire erosion causes and effects are hard to separate (Larsen *et al.*, 2009). It is stated by (Cerdà and Doerr, 2008; Woods and Balfour, 2008) among others that the characteristics of surface and soil in the immediate post-fire period are of critical importance for the hydrological response and erosion susceptibility of the burned catchment.

1.4 SIMULATION OF FIRE AND RAIN

To study the effects of fire on soil physical and hydrological processes a simulation is a suitable method to control as much as possible factors that might play a role. Fire as well as rain can be simulated under laboratory conditions. This enables testing the responses right after the fire and provides more rapid results than a natural and often unpredictable rainy season (Kukul and Sur, 2004). Besides, when done under laboratory conditions it also ensures replication of treatments of the fire and the rain.

With portable rainulators a rainstorm simulation can be done in the burned field (e.g. Rulli *et al.*, 2006; Johansen *et al.*, 2001; Cerdà *et al.*, 1997), but much simulation research is also done in the laboratory with smaller soil volumes, taken from the field in sections or prepared (e.g. Larsen *et al.*, 2009; Robichaud and Hungerford, 2000; Cerdà and Doerr, 2008).

The rainy season in the forest of Biriya provides annually around 650 mm of rain. Part of this rainy season can be simulated with a rainfall simulator, by simulating multiple rainstorms with a drying period in between. Apart from measuring the leading hydrological parameters during the simulated rainstorms, other measurements can be done which give an insight in the situation after and before a new rainstorm. During a rainstorm the soil volume under consideration can be seen as a 'black storage box' where water comes in and percolated water, runoff water and sediments come out. When all IN/OUT flows are checked the final balance must be zero.

This research focuses on the hydrological patterns of a forest soil after a fire. Like seen in previous research, fire can be simulated which enables precise recordings of the fire characteristics that are of key importance to ash formation, water repellency, organic matter combustion and cementing of aggregates.

The type of fire simulation of other research varies. Executed in the field and on a larger area, it is called a prescribed fire (Robichaud, 2000). Simulated in a laboratory implies that the simulation will be on small-scale and with more control of fire characteristics and surface features. Methods of burning that are reported range from using a propane heater (Robichaud and Hungerford, 2000), to placing the complete soil volumes in a oven at a high temperature (Doerr *et al.*, 2005). The simple method of manual burning was not published in international literature so far.

2. Objectives and research questions

The 2009 forest fires have damaged large parts of the soils and vegetation in the Peér'am catchment in the forest of Biriya, which has altered the ecological and hydrological conditions and the protection of the soil against overland flow and erosion. In the rainy season, during the winter period, the terrain is subject to heavy showers. Especially in the first season after the fire event, higher runoff rates compared to pre-fire conditions may be caused by intensified erodibility of the terrain. Simulating fire and rain in controlled experiments enables determination of changing runoff and erosion patterns as a result of successive storms, with and without ash cover. This information can be used to compare with observations in the burned-down forest of Peér'am catchment and predict the erodibility of patches of soil with comparable post-fire conditions, which contributes to increased insight in post-fire hillslope processes.

The research objective of this study is to:

Evaluate the short-term effects of wildfires on hydrological and erodibility parameters of forest soils, by laboratory simulations and field investigations.

To determine these effects the following factors will be examined at several moments in time, in both field and laboratory:

1. Soil water repellency:
 - a. Level and spatial distribution on soil sample surfaces
 - b. Level on surface and subsurface around trees in field
2. Runoff and infiltration responses to rain simulation of:
 - a. *Unburned* control soil samples, with and without vegetative cover
 - b. *Burned* samples, with and without ash cover
3. Vegetation and ash cover features of:
 - a. Burned soil sample surfaces
 - b. Selected field plots in sub- and intercanopy locations

The answers will be found measuring various parameters:

- Soil water repellency
- Spectral signature of surface
- Soil moisture content
- Saturated hydraulic conductivity
- Simulated runoff, drainage and sediment yield

3. Study area

The field experiments were conducted on a burned north-facing hillslope of the Peér'am catchment in the forest of Biriya, which is situated in the hills of Galilee, Israel (Figure 3). Originally, the area was occupied by maquis vegetation consisting of shrubs, and was heavily grazed. The Jewish National Fund (JNF) started in the 1950s afforesting the area, mainly with native and Mediterranean conifers (Ginsberg, 2006).

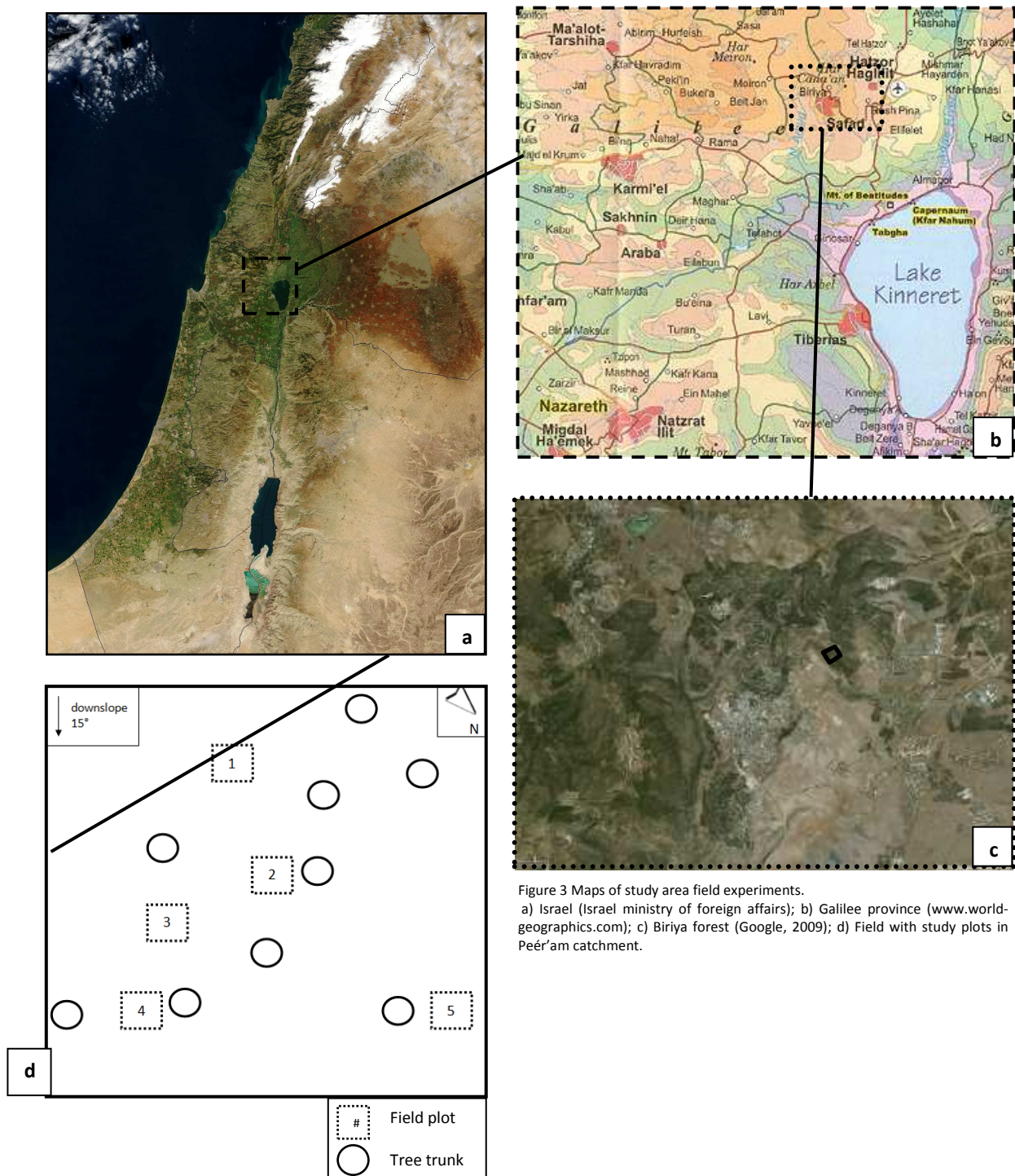


Figure 3 Maps of study area field experiments.
a) Israel (Israel ministry of foreign affairs); b) Galilee province (www.world-geographics.com); c) Biriya forest (Google, 2009); d) Field with study plots in Peér'am catchment.

The main vegetation present is *Pinus halepensis* with some oak (*Quercus calliprinos*) and herbs undergrowth. The bedrock consists of limestone and the dominant soil texture is clay loam. The annual precipitation is 712 mm (Har Kenaan (Zefat), Israel Meteorological Service, 2010) primarily falling in the winter period of November till February in moderate to heavy rainstorms. In the season 2008-2009 two events were recorded where >40 mm accumulated rain precipitated in one day, and an extraordinary maximum intensity of 58 mm h⁻¹ was recorded for a single one (Leska and Malkinson, personal communication). In general, events of 20-40 mm of accumulated rain for multiple days are occurring, where intensities reach maximal rates of 10-25 mm h⁻¹.

The summer 2009 wildfire destroyed all understorey vegetation and litter, scorching all trees and partly combusting entire trees. The organic layer was combusted leaving a white ash layer of 3-5 cm on the surface. According the classification of Ryan and Noster (as cited by (Keeley, 2009), Table 1) the fire was a moderate to deep burn, consuming all understorey plants and most needles, leaving white ash deposition and charred organic matter. Some trees were completely burned, leaving holes in the forest floor. During a field visit in November, 4 months after the fire, a several centimeters thick ash layer was observed in some places and the

holes of the tree roots were partly filled with burned litter and soil, indicating slope wash after the fire (Figure 4). The terrain without any vegetative cover, except remaining charred trees, had several small rills.

A field visit in January, 6.5 months after, revealed some sprouting of undergrowth vegetation (Figure 5). Some more rills were formed, however the thickness of the ash layer had not diminished.



Figure 4 Ash layer on mineral soil (top) and estimating depth of uprooted tree hole



Figure 5 Burned hillslope 8th of Nov, 2009 (left) and 17th of Jan, 2010 (right)

4. Methodology

Research has been executed (1) in the forest of Biriya and (2) in the laboratory of the Soil Erosion Research Station in Ruppin, Israel. The field was visited to acquire data on actual post-fire conditions in the winter season, such as water repellency, hydraulic conductivity, presence of ash and other surface and biotic characteristics.

On a section of the burned hillslope 6 plots of 1 m² were created: no. 1, 3 in a burned intercanopy location and no. 2, 4, 5 in a burned subcanopy location (Figure 3). Also, one control location (no. 6) was selected in an unburned area. The burned terrain has a gradient ranging from 15 to 20° and is facing northeast.

At first, the plots were meant for the field rainfall simulation, which eventually did not take place because of unexpected natural rainfall causing unsuitable field conditions. Hence, the simulation is executed in the laboratory.

4.1 FIELD EXPERIMENTS

5.1.1 Surface cover changes

To obtain information about the effect of the rains on biotic development and surface cover of the burned surface in the first wet season after the fire, the changes in surface cover features (vegetation, ash, exposed soil, charred material) are monitored by vertical photographs of the plots obtained 1.5 and 6.5 months after the fire from a height of 1.5 m. With supervised classification of ArcGIS Spatial Analyst, classified maps of the features are created for both dates.

4.1.2 Water repellency

One month after the fire the water repellency is tested on the floor surface and at 5 cm depth. For this purpose the Water Drop Penetration Time (WDPT) test was chosen, which involves placing a drop of water with a pipette on the surface where the litter and ash is removed. The time until complete infiltration of the droplet is measured and the procedure is repeated. The average of the three drops is taken and classified (Table 2).

Table 2 Classification Water Drop Penetration time test (adjusted to Tessler *et al.*, 2008)

CLASS NO.	MAGNITUDE OF WATER REPELLENCY	INTERVAL (s)
1	Wettable (hydrophilic)	≤ 5
2	Slight	6-10
3	Moderate	11-30
4		31-60
5	Strong	61-180
6		181-300
7	Severe	301-600
8		>600

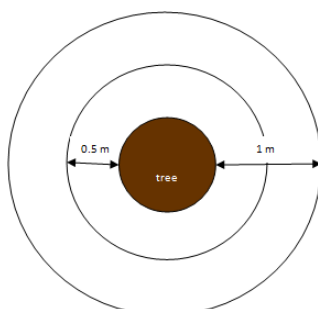


Figure 6 Schematic drawing of locations WDPT test in circles of 0.5 and 1 m around tree trunk



Figure 7 Hydrophobicity just below the ash layer in plot 4 (photo taken Nov, 2009)

The location of the drops is chosen in circles around some trees (on a distance of 0.5 and 1 meter from the trunk, Figure 6). The measurements are repeated 2 and 6,5 months after the fire, although the specific trees used for measurement were randomly chosen each time.

Samples of the studied soil are taken to measure gravimetric water content (dry weight loss), soil texture, OM content and in several cases pH, NO₃, NH₄, N and CaCO₃.

The soil moisture is determined by the dry weight loss method by means of drying for 24h in a normal heating oven at 105 °C. The soil chemical components are determined by a field service lab (Newe Ya'ar, Ramat Yishay).

4.1.3 Saturated hydraulic conductivity

By means of the Mini Disk Infiltrrometer of Decagon Devices[®] (Figure 8) we measured the saturated hydraulic conductivity (K_{sat}) of the soil surface of burned plots 1-5 and plot 6. K differs from infiltration rate in considering the cause of water seepage in terms of pull by gravity or hydraulic gradient and shows how quickly water will infiltrate when applied to a certain soil type (Decagon Devices). K_{sat} is obtained when all soil pores are filled. When soil dries out and the pores become filled with air, K becomes lower.

The tube-instrument with two water chambers is used to record the volume and

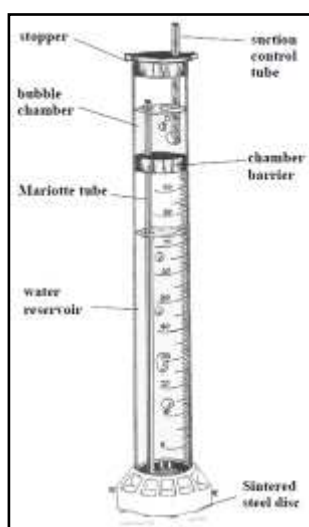


Figure 8 Mini Disk Infiltrrometer diagram (Decagon Devices, 2007) (left) and measurement in the field (right)

speed of water infiltration in 15.90 cm² area of contact with soil surface. Distilled water is used and a suction of -0.5 cm is used for the clay loam soil. As full contact between the disk and the soil is necessary for accurate measurement, fine sand is used to smooth the surface. The volume is recorded every 30 seconds for a period of 5 minutes. The hydraulic conductivity is calculated with a method proposed by Zhang (Decagon Devices, 2007). In this method the cumulative infiltration volume vs. time needs to be calculated and used in the following formula:

$$I = C_1 t + C_2 \sqrt{t}$$

In which C_1 and C_2 are parameters as C_1 is related to hydraulic conductivity and C_2 to soil sorptivity. C_1 is the slope of the cum. infiltration against the square root of time.

This C_1 together with van Genuchten parameter A (to obtain from a table in the manual, which takes the soil type, suction height and disk radius into account) is used in the following formula resulting in the hydraulic conductivity of the soil (k in cm/s):

$$k = \frac{C_1}{A}$$

The value of A given a suction of -0.5 cm on a clay loam soil is 6.0. Negative outcomes of k are not possible and indicate errors in the dataset, so they will be removed from the analysis.

Next to porosity and connectivity of macropores, K depends on soil moisture content and vice versa (Lebron *et al.*, 2007). Therefore, on every location in the field where a MDI experiment was carried out soil was collected, stored in airtight bags in a refrigerator with a temperature of 7 °C, sieved for 2 mm and measured for soil moisture content, using weighing and an oven treatment of 24 h at 105 °C.

4.2 LABORATORY SIMULATIONS

Since the field conditions were unsuitable for simulation of rainfall on the burned plots itself, the experiment was continued in the laboratory of the Soil Erosion Research Station (SERS). As transportation of blocks of burned soil to the laboratory would disturb the layers and surface irreversibly, unburned soil from another catchment in the same forest (distance 1 km) is taken to use for manual fire simulation.

4.2.1 Characteristics of soil and treatments

The actual bulk density of the soil cannot be determined, as the soil used for the experiment is disturbed during transport to the laboratory and by the preparation procedure. However, the disturbed bulk density can qualitatively be measured. The volume of a known weight of soil, sieved for the 4 and 15 mm fraction, is measured in a cylinder and the measurement is repeated three-fold. Next to this the porosity of the soil is determined, by the direct method of adding known volumes of water to the soil volume until the water tends to pond, as is in saturated conditions.

The aggregation of the soil is an important soil physical parameter as it influences soil erodibility, porosity of the soil and water infiltration capacity (Franzluebbers, 2002). An analysis of the composition of the soil gives insight in the general erosion sensitivity of the experimental soil.

The dry-stable aggregate size distribution was determined by placing in three repetitions a 500 g portion of soil on top of a nest of sieves, shaking for 10 min on a vibrating Sieve Shaker and weighing soil retained on the 2.0, 1.4, 1.0, 0.71, 0.5, 0.355, 0.25 mm screen and that passing the 0.25 mm screen.

To assign a weighing factor to the presence of aggregates proportional to their size Kemper and Rosenau (1986) proposed the mean weight diameter (MWD) which is equal to the sum of products of the mean diameter (x_i) of each size fraction and the fraction of the total sample weight (w_i) occurring in the particular size fraction, where the summation is carried out over all size fraction, including the fraction that passes through the finest sieve (Kemper and Rosenau, 1986):

$$MWD = \sum_{i=1}^n x_i w_i$$

Preparation

The unsorted soil was dried at 60 °C for 24 h and sieved in portions of two aggregate sizes: 0-4 mm and 0-15 mm. The sieving was executed to attain a fairly smooth surface and for the possibility to repeat the experiment. Two aggregate sizes were chosen to estimate differences in hydrophobicity for coarse and finer aggregates. The porosity and disturbed bulk density were measured, using the methods described by (Tan, 2005)

Trays (dimensions of 48x28x5 cm; 0.135 m²) were prepared for the burning and rainfall



Figure 9 Preparation of sample tray with gauze, gravel, geotextile and soil

simulation in the following way (Figure 9).

First the infiltration perforations in the left part of the tray were covered with a piece of gauze and a single layer of gravel to enhance the fast drainage of the infiltrated water out of the tray. Then the gravel was covered with a piece of permeable geotextile which was the base for the unburned soil. 10 trays were prepared, each carrying an approximate volume of soil of about 7 kg (Table 3). Four reference trays were included in the research: two with bare soil and two with bare soil plus a litter/needle cover.

Before the burn, the surfaces are tested for water repellency which is not detected.

4.2.2 Fire simulation

Except for the control treatments, the trays were subject to a burning treatment. Before each burning a thermocouple was installed with the tip of the sensor just below the soil surface at a distance of at least 10 cm from the boundaries of the tray, to enable measurements of the correct temperature on the soil surface.

This thermocouple measures the temperature of the air in the soil macropores, which is the air between the soil aggregates. After all litter was combusted the temperature was rising a little more, for approximately 30 min. The maximum temperature is recorded (Table 3).

Table 3 Characteristics of the experimental trays

CODE ^a	SOIL MASS (kg)	ORGANIC COVER ^b (g)	TREATMENT	BURNING TOOL AND DURATION (min)	T _{MAX} RECORDED ^c (°C)
4 -ash 1	6.9	400 +450	Burned; ash removed	20 - handheld gas heater	n.a. ^d
4 -ash	5.9	900+100	Burned; ash removed	15 - manual	280
15 -ash 1	8.8	400	Burned; ash removed	15 - handheld gas heater	285
15 -ash	6.9	900+120	Burned; not disturbed	13 - manual	300
4 + ash	7.8	800	Burned; not disturbed	20 - manual	170
15 + ash	5.8	900+130	Burned; ash removed	7.5 - manual	250
4 bare	6.4	-	Control tray, with bare soil		
15 bare	6.7	-	Control tray, with needles on top		
4 cover	6.3	100+120	Control tray; with bare soil		
15 cover	7.3	100+150	Control tray; with needles on top		

^a Code = [aggregate size, disturbed (-ash) or undisturbed (+ash); 'repetition']

^b Organic cover = material that was available for combustion: [dry needles + other plant litter (partly decomposed)]

^c Duration and tool for burning = active burning in minutes - way of burning

^d N.a. means not available data, as it is not recorded

Two trays are treated with a gas fired radiant heater and four with a manual burning treatment. Two parameters were used to set targets for the burns: complete combustion of all the organic material cover and a recorded temperature between 175 and 270 °C as it is shown in earlier laboratory research (Doerr *et al.*, in press) that hydrophobicity is intensified within this range.

Burning the material with the heater caused a fast and superficial burn which did not combust all the organic material, causing some distrust about the reliability of the method compared to actual forest fires. Therefore, the experiments burned with a propane gas heater (4-ash1 and 15-ash1) are omitted in the rest of the report, as the heated gas has other properties to change the surface of the soil than natural or simulated fire does. This was for example evident from the cemented aggregates which were seen on the surface of the treatments burned with the heater. The temperature of the gas was so high that the litter was extremely quickly burned, intensifying the temperature on the surface for only a very short period.



Figure 10 Procedure of fire simulation

The manual burn was done by lighting the needles at several places with matches and ensuring a moderately uniform pattern of burn (Figure 10). It gave slower ignition, but a longer period of high temperatures on the complete soil surface. Some extra charcoal was added to increase the heat of the fire. The air temperature during the fire simulations was around 23 °C. Fire was intensified using a ventilator and the organic material was stirred to have complete combustion of all the litter. In some cases maximum $T > 270$ °C are reached, by which hydrophobicity may be destroyed again due to the breakdown or volatilization of organic compounds (Doerr *et al.*, in press). However, in all cases the maximum temperature was only reached at the end of the complete burning procedure and did not persist for a long time.

The treatments with no ash (-ash) are prepared by blowing the superficial ash from the trays with a handheld fan. No raking is applied, as the tools would damage the soil surface (Figure 9). The burned trays are cooled to room temperature and stored in a dry place where no external disturbance could change the surface properties.

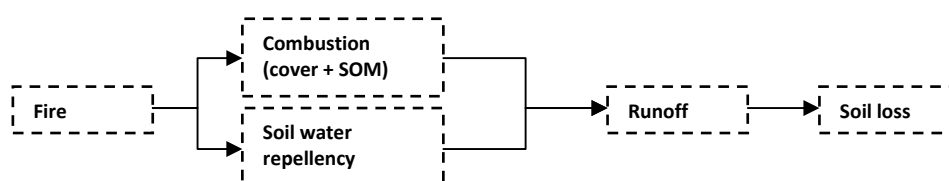


Figure 11 Simplified scheme of the chain of post-fire erosion processes during a rainy season

It is assumed that the fire has impact on several mechanism of the soil. During the experiment a certain order of measurements is applied which provides insights in the chain of processes (Figure 11). The influence of several side connections are to be considered, depending on the presence of an ash cap on the surface, crust formation, and spatially different drainage and runoff (sources and sinks, preferential flow). Links between the treatments are made considering this succession of factors.

Table 4 Timing of simulation and tests, in days after the burn

Code	WR1 ^b	ASD0 ^b	Run 1	MDI1 ^c	ASD1 ^c	Run 2	WR2 ^d	ASD2 ^d	MDI2 ^d	Cutting
4 -ash	1	3	4	8	7	8	7	11	13	13
15 -ash	1	4	4	n.a. ^e	7	8	8	11	13	13
4 + ash	n.a.	n.a.	2	n.a.	5	5	12	8	12	15
15 + ash	7	4	4	8	7	8	11	11	13	8 (partly)
4 bare ^a	n.a.	4	4	6	7	8	n.a.	11	13	13
15 bare ^a	n.a.	n.a.	1	4	4	4	n.a.	8	13	13
4 cover ^a	n.a.	4	4	n.a.	7	8	n.a.	11	13	14
15 cover ^a	n.a.	n.a.	1	n.a.	4	4	n.a.	11	13	14

^a control treatments are not burned, day '15+ash' received burn is taken as reference day

^b Water repellency test 1 and hyperspectral test 0 are executed before 1st rainfall run

^c Mini Disk infiltration test 1 and hyperspectral test 1 are executed after 1st rainfall run

^d Water repellency test 2 (except '-ash treatments'), hyperspectral test 2 and mini disk infiltration test 2 are executed after 2nd rainfall run

^e N.a. means not available data, as it is not measured

4.2.3 Water repellency

The WDPT test is executed on the *-ash* burned treatments by applying droplets in a grid-wise manner on the soil (Figure 12,13). As is stated by Doerr *et al.* (2005) a minimal period of 24h after the burn is needed for equilibration before WR can be tested, so the tests are executed the day after. Each 5x5 cm grid cell received 1 drop in each corner, giving a water repellency pattern of the surface with a spatial resolution of 2.5 cm.

Compared to what is done in the field, the water repellency is not measured in the deeper soil layers, as this would disturb the soil and make it unsuitable for a second rainfall simulation.

Two WDPT tests (WR1, WR2) were executed within several days after the burning on the surface of each treatment, after the first rainfall simulation and in several cases after the second rainfall simulation (Table 4). To ignore border and corner effects of the fire the outer grid cells were not used for measurement, which resulted in placing drops in the 32 remaining grid cells (Figure 12). Each 5 cm grid cell received 3 or 4 drops, which served as repetitions.

The *+ash* treatments received no WDPT test before rainfall run 1. And when eventually tested, the remaining ash layer was gently removed on the places where the drops were placed. The time till complete infiltration was measured, with a maximum recording time of 5 minutes. The data were categorized by the same classification as used in the field (Table 2) and were mapped in ArcMap.

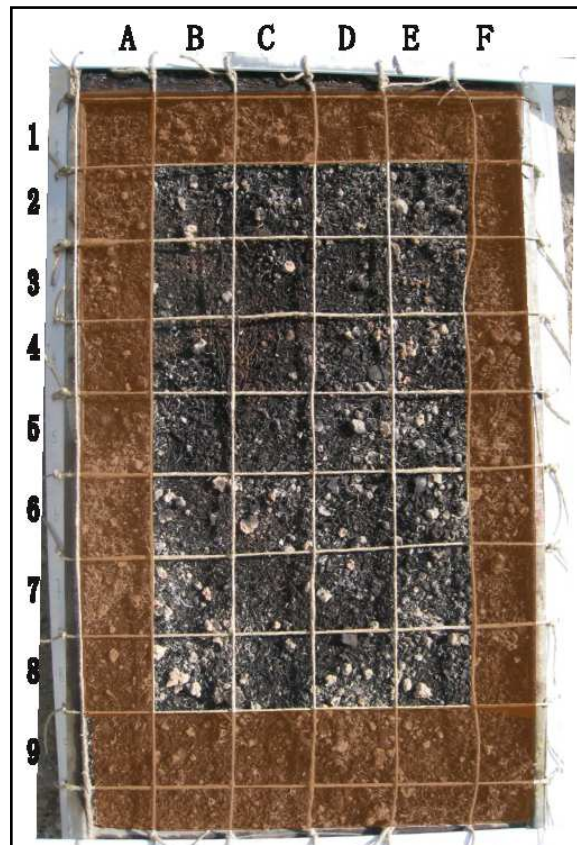


Figure 12 Grid for WDPT test; shaded area is not measured

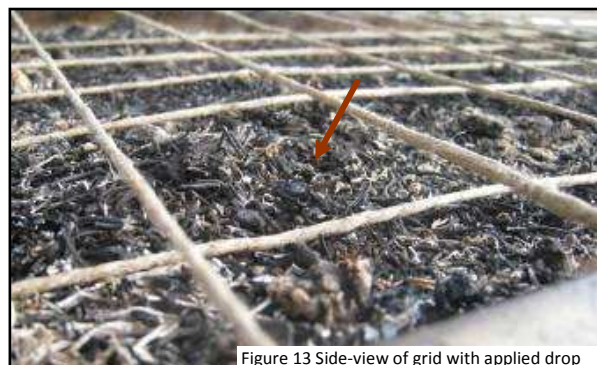


Figure 13 Side-view of grid with applied drop

4.2.4 Rainfall simulation and analysis

The simulation of the site-specific rainfall on the treatments was executed with a rotadisk nozzle-type rainulator, placed in the laboratory of the Soil Erosion Research Station (SERS), Ruppin, Israel. The drops from the nozzle, which produces a drop distribution that includes a large number of sizes, reaches the experimental boxes through the aperture in the slotted metal disk that rotate on a vertical axis beneath the nozzle (Morin and Cluff, 1980).

The boxes were placed on a carousel beneath the rainulator at a 5% slope, 5 per run (Figure 14). During the run they rotated anti-clockwise beneath the nozzle of the rainulator. Tap water was filtered to produce distilled water which was transported to the basin on top of the rainulator with a steady pressure. During the experiments it was checked that the pressure remained stable

and the water maintained an EC-value of 0 mS cm^{-1} , to see the EC-change in the drainage water and to avoid dispersion of the clay minerals which would too quick form a impermeable crust.

The speed of the rotation was recorded by electronic devices, so with the known rain volume (148 mL) and the rotation time (113 sec/lap) the rain intensity could be defined. The system was validated by two test runs in which the received rain in each tray was collected. The test runs

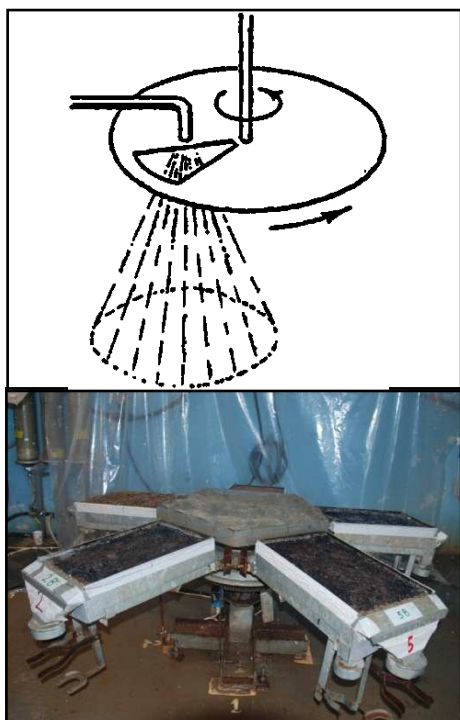


Figure 14 Working principle of rotadisk rainulator (top: Hudson, 1993; bottom: Eli Argaman, 2010).

took place before and after the series of simulations. Out of the results it was concluded that the system was quite consistent and that the rainfall intensity ranged between 32 and 33 mm h^{-1} .

At the lower end of the box a trough collected the runoff (R) and sediment, but did not capture the water and sediments lost over the side by rain splash erosion. At the lower end there was also a outlet which collected the drainage water (D) that percolated through the soil volume, the gauze and gravel. D and R

were collected in vessels and cylinders, and volumes were recorded in equal intervals: D was measured in the 1st, 3rd, 5th etc lap, R in the 1st + 2nd, 4th + 5th, etc. lap for each tray. For total volumes of D and R the data were interpolated.

At the starting and final laps of each run the EC of the drainage and runoff water was measured with a hand-held ECTestTM High Waterproof meter with a

resolution of 0.10 mS cm^{-1} and an accuracy of 1% (Eutech Instruments). Approximately half of the collected runoff volumes is stored in clean and

weighted cans, which are dried for 48h at 40°C . The cans with the remaining sediments are weighted and the sediment yield is calculated. About one-fifth of the stored sediment portions are taken out of the cans with a brush and stored in little glass vessels. If possible, these samples will be used at a later stage for laboratory research on organic matter, mineral content and ash composition and fraction. These results will not be presented in this report.

Each set of 5 treatments received two rainfall runs separated by a drying period to simulate part of a Mediterranean rainy season. Between the simulations the trays are dried in a stove at a temperature of 40°C , to avoid too fast shrinking of the (clayey) soil. It is assumed, although not checked, that the shallow soil profile is completely dry at the start of the second rainfall run.

Due to the shrinking and cracking of the surface after the first run, the trays need some special preparation before the second rainfall run. The openings which where formed between the soil and the bottom were sealed with fluid silicon sealing material.

The duration of the first rainfall run was 4,5 hours, due to the purpose of reaching an equilibrium in throughflow for the whole set of treatments in the simulator. For the 2nd, 3rd and 4th run it was decided to quit the simulation after 2 hours, even if at that moment the final infiltration rate (= final erosion rate) was not attained.

4.2.5 Saturated hydraulic conductivity

The saturated hydraulic conductivity of the soil samples is analyzed to be able to compare the rates with field conditions and with the (final) infiltration rates during the rainfall simulation.

MDI1 is executed after rainfall run 1, MDI2 after the second, both after a drying period of at least 3 days (Table 4). A small amount of sand is used for smoothing the surface, but due to the

organic matter cover and the wish not to disturb this too much not all treatments received 2 or 3 repetitions. Where possible a repetition was executed on the top, middle and bottom part of the tray. In case of needle cover, the needles were temporarily removed to create a bare surface large enough for the infiltrometer. Cumulative infiltration data were analyzed using the formula given by the designer.

The second MDI experiments on the laboratory trays were also accompanied by soil moisture measurements, as moisture content is a major factor in conductivity of water. On every tray two small samples were taken and put in an oven at 105 °C for 24h.

4.2.6 Hyperspectral sampling

The surface of the trays is sampled with the ASD Portable Field Spectrometer (ASD Inc.), which is able to measure the spectral radiation in the VIS, NIR and SWIR electromagnetic region (350-2500 nm) with sunlight or artificial lighting. The measurements are done with a 1.5 m optic fiber which is connected to the detectors in the spectroradiometer. The spectral wavelength range is covered by three sensors, each with a specific spectral range.



Figure 15 High Intensity Contact Probe (ASD Inc.)

Before each series of measurements, an optimization is made to ensure an optimal connection between the sensors. After that, the system is calibrated with a white reference: a straight line close to 100 % reflection means a high accuracy as all light is reflected.

A notebook with RS3™ software (ASD Inc.) is connected to the spectroradiometer and receives and displays the data in a spectral signature graph. The noise in the edge areas of the three detectors of the spectrometer (1.35-1.4, 1.78-1.95; 2.45-2.5 μm) is smoothed by an operation in RS3™ and in some cases removed in Excel.

At the start of the experiment, right after the burn simulation, all trays were measured outdoors with sunlight and average humidity (75%). Due to clouds and high humidity later at the experiment the next measurements are executed with the optical fiber inside the ASD High Intensity Contact Probe which uses halogen light with a spot size of 10 mm diameter (Figure 15). This probe is placed loosely on the surface (needles, ash, soil crust) for several seconds equilibration, after which the point measurement is made. Placing the probe not completely on the surface will effect the reflectance values due to 'leakage' of light. Every tray is divided into 5 sections (Figure 16) where three repetitions of the point measurements are executed. Each tray is measured 3 times: after the burn, after the first rainfall simulation and after the second rainfall simulation. So in total there are 45 spectral reflectance curves per treatment.

The data are transferred to ASCII files, averaged per part and further analyzed in Excel. It is checked whether the spectral signatures of the fractions are valid for the whole surface and first estimates are made about differences in absorption features of minerals and organic matter.

In a later stage, which is beyond the scope of this research and subsequently will not be described, the charts will be quantitatively analyzed for ash, mineral and OM content and characteristics.

The spectral signature of every object is largely influenced by the moisture content, as visualized in the drops in the curve due to water absorption. Therefore, of four trays several small soil



Figure 16 Subdivision of surface into 5 sections where each 3 spectral signatures are taken.

samples are taken of the surfaces and oven-dried at 105 °C for 24h to examine for moisture content.

4.2.7 Sections of soil sample volumes

To examine the effects of the rain on the soil physical characteristics throughout the soil profile, the soil volumes are cut after the last rainfall run to provide profiles (top, middle and bottom) and horizons sections (crust, middle and lower) (Table 4). The 'cakes of soil' are categorized per treatment and stored on trays in a storage room with ambient temperature.

High-resolution pictures (300 dpi) are taken to capture presence and forms of features in the profiles and layers: cemented soil particles, ash accumulation and percolation, presence of OM in the deeper layers, ash layer on the surface. Secondly, the water repellency on top of the cut horizons is tested with WDPT.

4.3 ANALYSIS

Water repellency lab

To predict preferential flow patterns and flow accumulation due to water repellency on the experimental soil samples, an ASCII file was made of the values of WR, slope and border according the algorithm:

grid value = WR level + height related to bottom (=1) and considering a slope of 5% (=slope during rainfall run)

The border cells got a value +0.1 to prevent the model from computing outflow from the sides of the plot. With Hydrology algorithms of the ArcMap Spatial Analyst Tools the Flow Direction and Flow Accumulation is computed for each treatment. The output maps show grid wise preferential patterns of flow, which are visually compared with the patterns of ash, combusted organic material and bare soil in the pictures.

Hydrologic responses

The measured volumes of runoff and drainage were used to calculate runoff and drainage rates per time unit, final rates and runoff coefficients. The sediment yield is converted to a unit appropriate for this scale ($\text{g m}^{-2} \text{min}^{-1}$) and the percentage of sediment in the runoff volume (sediment runoff ratio in $\text{g L}^{-1} \text{min}^{-1}$) is calculated. Also, initiation times of drainage and runoff are processed.

Next to that, the measured EC values of the runoff and drainage water is analyzed to identify drainage patterns of organic matter and minerals.

Statistical analysis for significance and correlation between the treatments is not applied, due to few data sets and no replications.

5. Results

5.1 FIELD EXPERIMENTS

5.1.1 Surface cover changes

The burned hillslope received in the period between November (+4 month) and January (+6 month) enough rain (> 200 mm) and radiation to let the biotic environment re-establish. On the intercanopy plots 1, 3 and 5 the first plants (surface cover of 4%) are resprouted after 6 months, while they were hardly present at the start of the rainy season, 4 months after the fire (Table 5; Appendix I).

For the subcanopy plots the vegetation regeneration process is somewhat slower with no aboveground growth within 6 months after the fire.

Table 5 Fraction of surface cover features field plots 1-5 at moments 4 and 6 months after the fire (%) Appendix I

plot	INTERCANOPY						SUBCANOPY			
	1		3		5		2		4	
# month after fire	4th	6th	4th	6th	4th	6th	4th	6th	4th	6th
soil	17	17	26	35	8	17	15	12	15	25
stones			9	11	3	4	8	6		
charred material	83	82	64	46	55	63	53	47	50	44
ashlayer					33	10	24	25	35	30
vegetation	0	1	1	8	0	3				
unclassified	0	0	0	0	1	3	0	10	0	1
TOTAL	100	100	100	100	100	100	100	100	100	100

In all plots the fraction cover of the non fire-related components (unburned soil, stones, vegetation) increases during the rainy season, and the reverse is happening for the percentage of surface covered by burned organic material. For the ash layer on the subcanopy however the surface cover is not or only slightly decreasing. While on the intercanopy plots there was no thick ash crust initially (if there, blown or washed away in months directly after the fire) or decreased largely (plot 5). Striking is the plot (3) without any ash where the vegetation is resprouting most, which might be due to fast light interception of the sprouts.

5.1.2 Water repellency

At three moments after the fire the water repellency of sub- and surface is measured, in two circles around randomly selected trees. 20% of the recordings in the control soil have strong WR levels, but no severe WR is found (Figure 17b). The soil water repellency is not different for the sub- and surface of the control area.

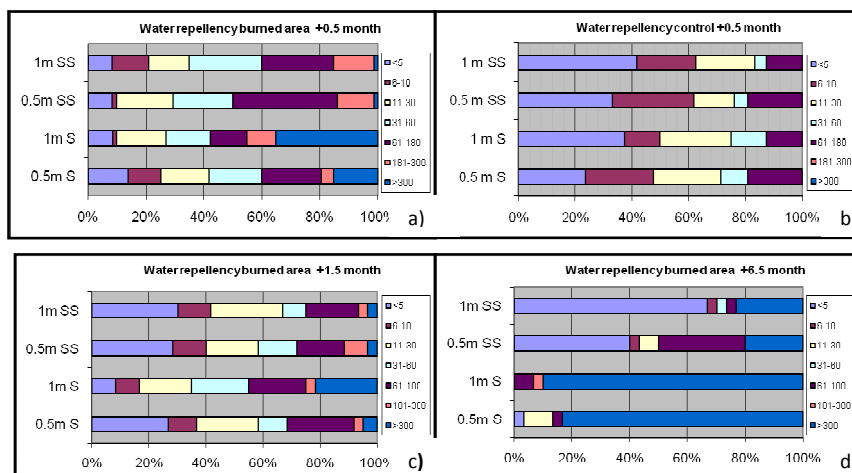


Figure 17 Soil water repellency level and occurrence in burned field and control (b): 0.5 (a), 1.5 (c) and 6.5 (d) months after the fire. S = surface; SS = subsurface, 0.5 or 1 = 0.5 or 1.0 meter from a burned tree. < 5 = wettable; 6-10 = slight; 11-60 = moderate; 61-300 = strong; >300 = severe.

Strong and extreme WR levels (>60 s) are measured two weeks after the fire in 40-60% of the cases and the occurrence diminishes in the following month, especially for the subsurface (Figure 17a,c). Half a year later however, extreme WR is greatly present in the subsurface at both distances from the tree and it has also increased dramatically on the direct surface of the tree (Figure 17d).

5.1.3 Saturated hydraulic conductivity

Values of K_{sat} differed considerably between and among the sub- and intercanopy plots (Table 5). On average the intercanopy plots have lower K_{sat} (11.6 mm h^{-1}) than the subcanopy plots (18.5 mm h^{-1}). The average burned K_{sat} is ~ 5 units lower than the values measured on the control, but because of the large extreme values the difference is not statistically significant. From the data it can be concluded that water infiltration in the surface of the burned soils is slower, especially where ash is considerably removed. A difference in penetration resistance between the sub and intercanopy positions is not recorded, so no relation between compaction and position in the burned field can be established.

Table 6 Saturated hydraulic conductivity, soil moisture and penetration resistance of the study plots soil surface, 4 months after the fire.

Plot no.	position	angle °	Ksat (mm h^{-1})				average soil moisture	penetration resistance surface (kg/m^2)
			a	b	c	average		
1	inter	9	2.4	19.8	6.0	9.4	32	0.5
2	sub	10	8.4	n.a	n.a.	8.4	23	1.0
3	inter	9	19.2	13.2	9.0	13.8	32	0.4
4	sub	15	11.4	12.0	45.0	22.8	27	0.1
5	sub	8	28.8	24.0	19.8	24.2	25	0.4
6	control	22	12.0	43.2	13.2	22.8	33	0.5

5.2 LABORATORY SIMULATIONS

5.2.1 Soil characteristics

The texture of the used soil is clay (25 % sand, 30 % silt, 45 % clay) with a pH of 7.5, an EC of 0.65 dS/m and organic matter content of 1.02%. The fine-grained type is close to terra rossa, which are typical Israeli soils, formed by weathering of carbonate sedimentary limestones and containing many carbonates and iron oxides.

The disturbed bulk density of the soil is approximately 1.08 g mL^{-1} . The porosity is 49 % for 15 mm and 56 % for 4 mm aggregate size samples. The average mean weight diameter is 0.88, indicating that larger aggregate sizes are present in larger amounts in the soil (Figure 18).

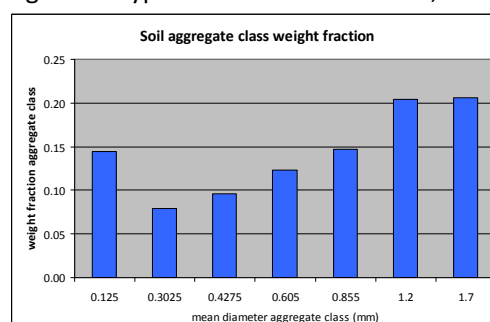


Figure 18 Weight fraction of each aggregate class in the sampling soil

The soil volume in each box ranges between 5.8 and 8.8 kg. For the 4 mm aggregate size portion the average volume is 6.7 kg, while for 15 mm it is 7.2 kg. However, by the method of preparing the sample and skimming of all loose material, it is ensured that each treatment has a comparable smoothness, depth of the soil profile and distance between the soil surface and the edge of the box.

5.2.2 Fire simulation characteristics

The fuel load that is used for each fire is 1.0 kg for all treatments, except for *4+ash* which is covered by 0.8 kg of needles and litter. The fuel load has the same components for every treatment and the amount is added in parts to the fire.

The time the flames of the fire need to combust all litter until it is ash or glowing material is varying, depending on variables as fuel load and composition, wind strength and direction, places of ignition among others.

The cover on the cover control treatment is not burned and limited to 0.25 kg as the boxes can not hold more.

5.2.3 Water repellency

Water repellency is tested twice: before and after the first or second rainfall simulation. Thus, the effects of the burning and the first rainstorm simulation of 2h with constant rain intensity of 33 mm/h can be examined by analyzing qualitative (WR level and relation with surface characteristics) and quantitative (amount and spatial distribution of cells with WR) differences.

An integration of the qualitative and quantitative data on water repellency can be done by calculating an average level of WR for the whole sample surface, which is defined by WR levels present and the number of grid cells as the weighing factor. Accordingly, the average level for *15-ash* and *15+ash* decreases from 1.48 to 1.23, resp. 1.49 to 1.02. Class 1 means a wettable soil (hydrophilic) so the higher the value, the more cells exist with some level of WR. Where the presence of WR is largest on both treatments after the first rainfall simulation, the surface of both trays are more or less hydrophilic after the second rainstorm.

For *4-ash* this is the reverse, as the average level increases from 1.07 to 1.28. Due to no available data of WR1 for *4+ash* the difference can not be displayed. The results of WR2 of this treatment however show much more cells with some water repellency than *4+ash*, even after 2 rainstorms. The treatment with the highest water repellency is *15-ash* during the first WDPT test, which has some grid cells classified as strong/ severe. The second test and the tests on all other treatments reported sporadic moderate-strong water repellencies, while most cells did have slight or no water repellency.

Table 7 Frequency of water repellency levels for 2 WDPT tests (in # of grid cells)

TREATMENT		4 - ash		15 -ash		4 + ash		15 +ash	
WR test ^a		1	2	1	2	1	2	1	2
WR LEVEL	1	117	96	102	108	n.a.	106	86	54
	2	3	11	10	13		12	19	1
	3	3	2	8	6		2	12	0
	4	0	1	3	0		0	3	0
	5	0	1	2	0		0	0	0
	6	0	2	1	1		0	0	0
	7	0	0	0	0		0	0	0
	8	0	0	2	0		0	1	0
average level		1.07	1.28	1.48	1.23		1.13	1.49	1.02

^a 1 = hydrophilic, 2 = slight, 3-4 = moderate; 5-6 = strong and 7-8 = severe

An observation was made concerning the trays burned with the heater as they showed more cells with strong-severe WR than manually burned (not presented in Table).

The position of the grid cells with surface water repellency is not uniform for all treatments (Appendix II). The map of WR1 on *4-ash* shows occurrence along the centre line, where fire temperatures are assumingly highest. While the levels are higher during WR2 on the same treatment, the water repellent area are only present in the bottom part of the tray.

For *15-ash* the pattern is different, as the WR cells occur for WR1 as well as WR2 on the sides of the tray.

For the undisturbed cases (*+ash*) the water repellency cells are more evenly spread over the trays. As WR2 *15+ash* was done after primary cutting of profiles, most of the cells received value 0 = no data (Appendix II).

Overlays are created of the preferential flow patterns, modeled using the places on the trays where water repellency is occurring on the surface, with the photos made of the trays (Appendix III). As *4-ash* had water repellency in the centre, first along the whole line and later only on the bottom, the preferential flow is modeled on the sides. As is seen on the feature maps (Appendix IV) all the ash and blackened soils is removed by the first rainstorm. On the bottom however, remained charcoal and burned organic material, which can explain the maintained WR there. The preferential patterns of flow clearly surround this impermeable soil surface.

The flow accumulation is highest for *15-ash* in the first run, as the water repellency is severest and subsequently less water can infiltrate. This may explain why between the classified maps of run 1 and 2 there such a difference in cover. Most of the burned soil is washed off, leaving exposed unburned soil and organic material which is not completely combusted. Especially for run 2 the streams are modeled to be concentrated in the centre bottom part. Apart from the modeled flow that tends to follow the same path as a major crack, there are no apparent spatial differences in the surface features of the photo and classified map.

The difference in surface cover between *4+ash* and *15+ash* is clearly visible as more organic material remained on the soil of *15+ash* after two rainfall runs. The stream pattern for *4+ash* WR2 shows no clear preferential flow, apart from a slightly larger accumulation on the left side, corresponding to more exposed soil on that side.

The water repellency of the deeper layers is not measured before the rainfall simulation, but it is tested on top of the cut horizons. Apart from slow infiltration on the crusts, no water repellency is detected for the lower layers.

5.2.4 Hydrologic responses rainfall simulation

Infiltration and drainage

The initiation time of complete throughflow is for both rainfall runs not completely similar for all burned treatments. For run 1 it starts, except for *15+ash*, after 20 mm of received rainfall. In the second run this fairly sooner, where only 14–19 mm is needed to drain completely through the whole profile.

For the first run the drainage patterns of the treatment types can be divided into several groups (Table 8; Figure 19):

- Steady high drainage rates ($\sim 33 \text{ mm h}^{-1}$) for the treatments with complete soil cover by needles. For *4 cover* the rates fluctuate at the start of the rainstorm but after 50 mm cum. rain keep a steady level. The drainage level is equal to the precipitation rate of the simulating, indicating the absence or petite amount of runoff potential.
- Decreasing drainage rates for all the burned treatments. At the start the level is equal to the attained infiltration of the cover treatments (33 mm h^{-1}), but the higher the amount of rain received, the lower the drainage rate. The linear drop in drainage level is not similar for all treatments: this is approx. 0.20 mm h^{-1} per mm for the *+ash* treatments, but 0.40 resp. 0.57 for *15-ash* and *4-ash*. The latter tends to flatten towards a steady drainage rate of 7 mm h^{-1} after 65 cum. mm, but the other treatments did not attain a steady final infiltration rate at the end of the rainfall run. As *4+ash* was included in run 1 the curve extends beyond 80 mm and it is observed that eventually this treatment reaches a steady final infiltration rate of 18 mm h^{-1} .
- Steady low drainage rates for the bare soil treatments. Striking is the difference in behavior as *15 bare* has an initial drainage rate of 5.6 mm h^{-1} after 25 cum. mm but drops in several laps to a steady level of 1.5 mm h^{-1} . Treatment *4 bare* however, attained much later, at 53 cum min, complete throughflow and it started with the

lowest drainage rate possible. In a short time is rose to the same drainage level as *15 bare*.

Table 8 Runoff and erosion data of the rainfall simulation experiments

SAMPLE		4-ASH		15-ASH		4+ASH		15+ASH		4 BARE		15 BARE		4 COVER		15 COVER	
Rainfall run		1	2	1	2	1	2	1	2	1	2	1	2	1	2	1	2
Duration (min)		153	119	153	119	265	126	153	119	153	119	265	126	153	119	265	126
Final cumulative rainfall (mm)		88	65	88	65	145	70	88	65	88	65	145	70	88	65	145	70
Cum. rain till runoff initiation (mm)		17	7	14	7	13	7	19	7	14	7	13	7	14	7	13	7
Cum. rain till drainage initiation (mm)		23	14	23	10	26	18	18	10	54	66	26	43	26	10	26	14
Final infiltration rate (mm h ⁻¹)		7,1 ▼ ^a	2.2	11,5 ▼	3.4	18	6.8	20,1 ▼	5.8	1.5	0	1.6	1.6	33.4	33.3	32.6	32.6
Runoff rainfall ratio		2.72	3.90	1.99	3.83	0.37	3.93	1.35	4.09	5.44	4.52	4.12	4.43	0.03	0.04	0.10	0.10
	increase (%)		144		193		105		302		83		108		124		99
Final runoff rate (mm h ⁻¹)		23 Δ ^b	25	21 Δ	25	12	21	14 Δ	24	25	23	28	24	0.2	0.2	0.8	0.6
SY average (g mm ⁻¹ of rain)		1.16	2.00	1.22	2.54	0.55	2.30	0.61	2.16	3.57	5.67	3.63	3.29				
SY max (g mm ⁻¹ of rain)		1.99	3.49	2.75	3.35	0.81	3.28	1.02	3.19	5.13	6.94	6.17	4.29				
Sediment runoff ratio (g L ⁻¹ mm ⁻¹ of rain)		1.57	2.54	2.38	2.44	0.43	2.84	1.32	2.41	3.72	5.47	3.40	10.74				
Initial EC value (mS)	drainage	2	0.2	2	0.3	1.7	0.4	1.7	0.5			0.4	0.2	1.1	0.4	0.7	0.5
	runoff	0.2	0.1	0.3	0.5	0.6	0.3	0.4	0.3	0.3	0.1	0.4	0.3			0.3	0.5
Final EC value (mS)	drainage	0.3	0.3	0.3	0.4	0.4	0.3	0.3	0.4			0.5	0.8	0.2	0.1	0.3	0.1
	runoff	0.1	0.1	0.1	0.1	0.1	0.1	0.1	0.1	0.1	0	0.1	0.1			0.1	

^a Δ = rate still increasing;

^b ▼ = rate is still decreasing

The drainage hydrographs of the next rainfall run show different patterns. The control treatments with cover behaved comparable with the first, but the burned plots showed completely different infiltration graphs (Figure 20). Already established during the first rainfall run and continued in the second, crust formation plays a large role in the infiltration potential of the surfaces.

The difference in the magnitude of the decrease in infiltration rates between the burned treatments is not clearly visible. All burned trays start draining between 14 and 19 mm accum. rain and rise to maximum levels around 10 mm h⁻¹, 60% lower than the initial conditions of run 1. That level is not reached by *4+ash*, which stabilizes at 6.5 mm h⁻¹. The drainage levels of other burned treatments drop at different speeds to lower stable levels: *15+ash* joins *4+ash* at 6.5 mm h⁻¹, while *4-ash* and *15-ash* have final infiltration rates of 2.2 resp. 3.5 mm h⁻¹. the curve of *4-ash* shows a sudden drop at 38 mm, which is also identically transposed in the runoff curve (Figure 20). Compared to run 1, all treatments reach in run 2 a steady final infiltration rate within the simulation duration of 80 mm.

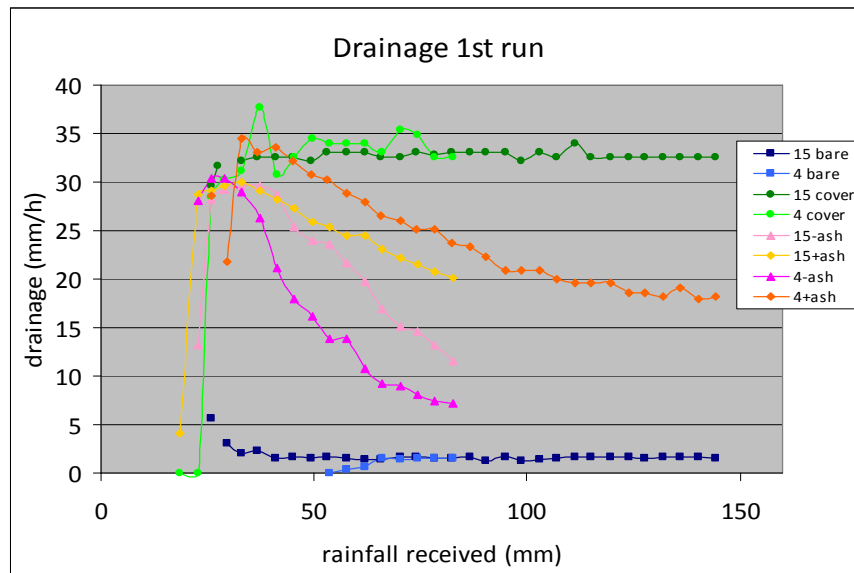


Figure 19 Drainage patterns (in mm h^{-1}) during the first rainfall simulation run

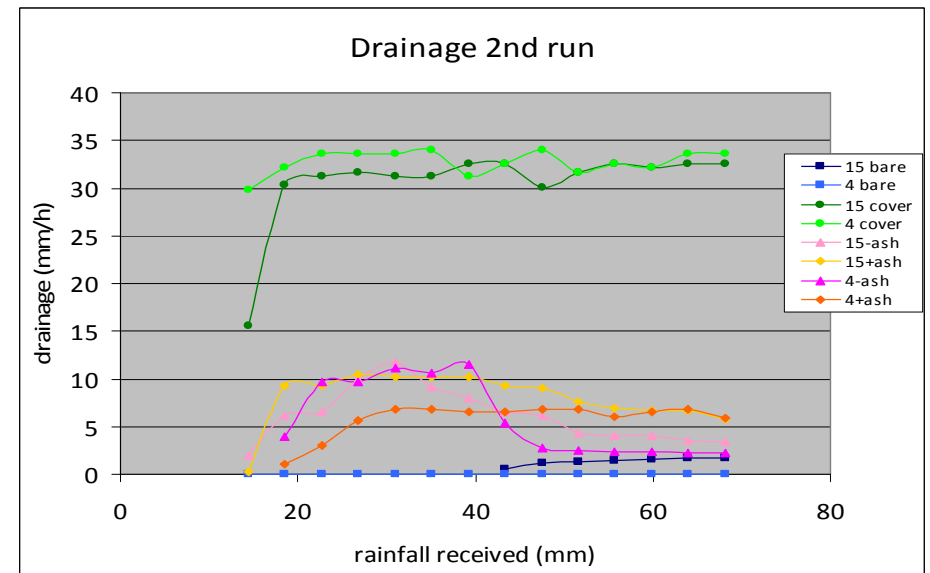


Figure 20 Drainage pattern (in mm h^{-1}) during the second rainfall simulation run

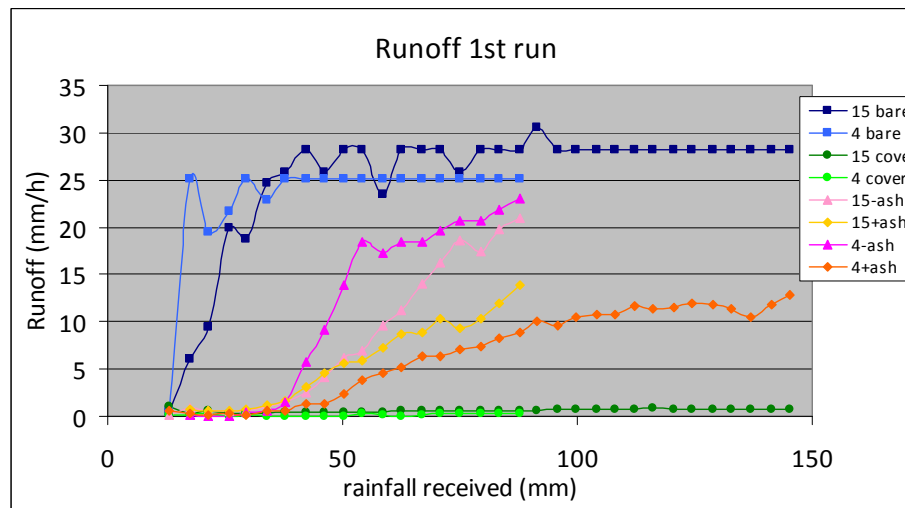


Figure 21 Runoff patterns (in mm h^{-1}) during the first run

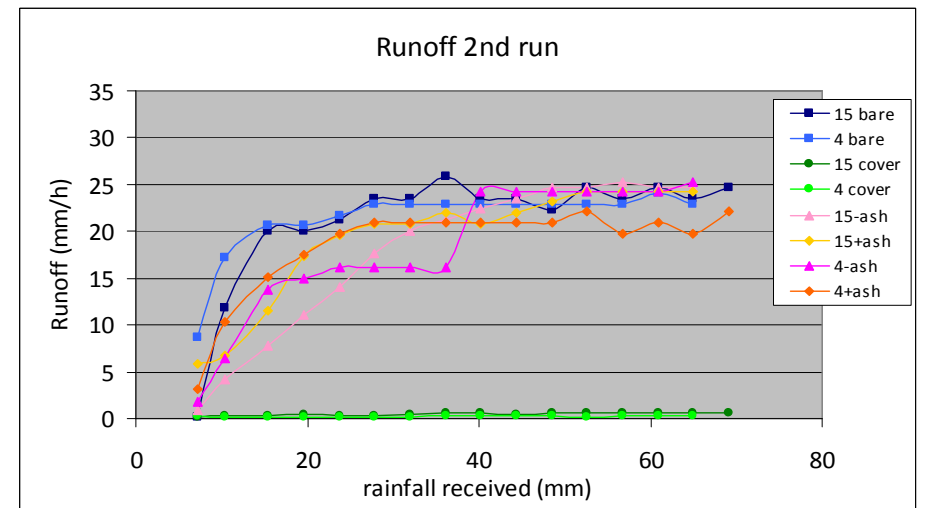


Figure 22 Runoff patterns (in mm h^{-1}) during the second run

Runoff

As expected, the runoff curves on the trays tend to be the opposite of the drainage curves, at least in terms of rates. The initiation of runoff is earlier than drainage for all treatments and both runs (Table 8). For all treatments, burned and control, runoff starts in run 1 when 13 to 16 mm rain is received.

In the first run there are again three groups to distinguish (Figure 21):

- A steady high level of runoff (25 and 28 mm h⁻¹ for *4 bare* resp. *15 bare*) which is reached after a period of 40 mm in which the runoff increases. The curve of *15 bare* is somewhat less stable during the first half of the run, which can be due to measurement errors (as it is first experiment).
- Increasing medium runoff rates for the burned treatments. After a period of very low runoff rates the surfaces start (at 35 mm) to hamper drainage (Figure 19) and runoff increases, with different speeds as was already reflected in the drainage patterns. The increase is approx. 18 mm h⁻¹ per mm for +ash, but 0.38 resp. 1.02 (and later 0.14) for *15-ash* and *4-ash*.
- Low runoff levels for the samples with needle cover, where on average 0.5 mm h⁻¹ water runs off.

Looking at the second run, from the drainage pattern it can be concluded that a change in runoff rates is expected. Transportation of water and sediments is created from the 7th mm of received rain on all the treatments. For *4 and 15 cover* the level remains at the stable low level of 0.5 mm h⁻¹, but the bare and burned treatment levels rise to 20-25 mm h⁻¹. Like in drainage, there is not much differentiation between the burned surfaces. The bare surfaces show the quickest rise in runoff and attain (after 30 mm rain) steady high runoff rates. In the second hour of simulation 2, this high level of runoff is also attained by 3 out of 4 burned surfaces. Notice the slightly lower runoff rates of the bare treatments compared to run 1.

Sediment yield

The values of the sediment yields over the complete first rainfall run can be divided into four groups (Figure 23, Table 8):

- high soil loss rates on the bare control treatments, reaching average levels of 3.6 g mm⁻¹ of rain and maximum levels (on *15 bare*) of 6.2 g mm⁻¹ of rain.
- medium levels of soil loss on burned -ash treatments, with averages of 1.2 g m⁻² min⁻¹ and maximum soil loss rates of 2.8 g mm⁻¹ of rain.
- lowest soil loss levels are realized on the undisturbed treatments where the ash protects the soil against erosion. This pattern is also corresponding to the lower runoff values in the first rainfall simulation. The average soil loss rate is 0.6 g mm⁻¹ and it reaches at the most (for *15 +ash*) 1.0 g mm⁻¹ of rain.
- no soil loss on the trays with complete soil needle cover (*4 and 15 cover*)

Another difference is the course of sediment yield over time. While for the *bare* and -ash treatments the soil loss rates increase with precipitation, the rain on the ash-covered treatments produces a relatively low soil loss rate, which does not rise over time (Figure 23). Corresponding to the initiation time of runoff, the bare treatments show soil wash within the 20 mm cum. rain, while the burned treatments start later with 38 and 46 mm for the -ash cases and 46 and 72 for the +ash cases. A equilibrium soil loss rate is reached for +ash after 30 mm of runoff, for the other cases the erosion is not stabilized in the course of the simulation.

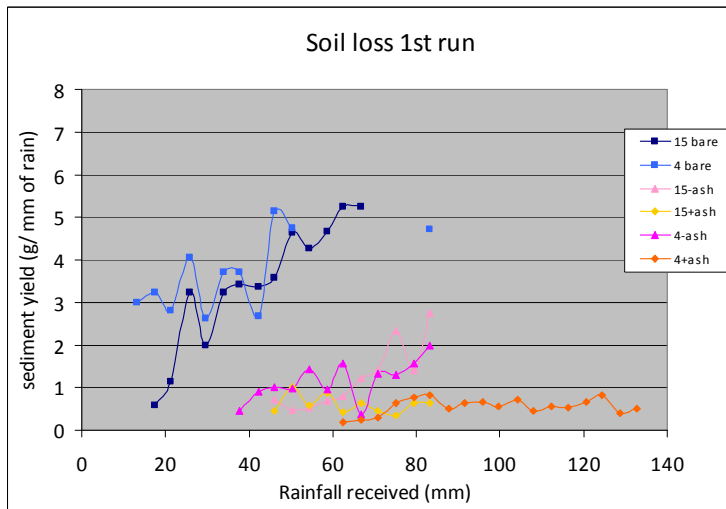


Figure 23 Sedigraphs of the first rainfall run for all burned and bare treatments
(the duration of the curve of 4+ash continuous, because rainfall run 1 took twice more time)

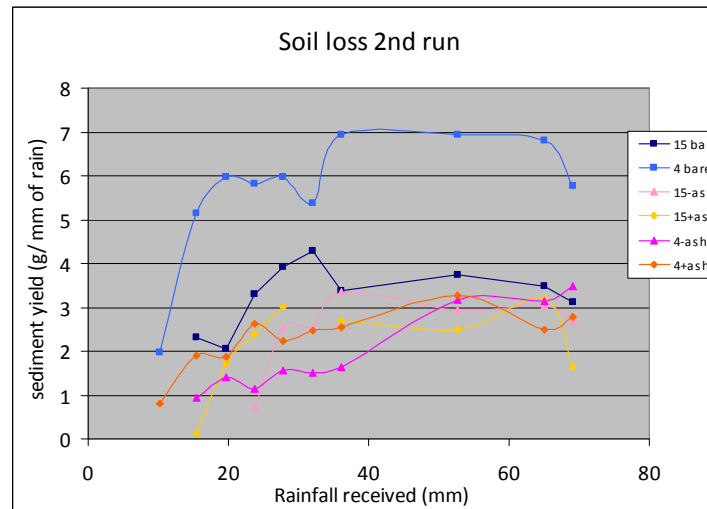


Figure 24 Sedigraphs of the second rainfall run for all burned and bare treatments

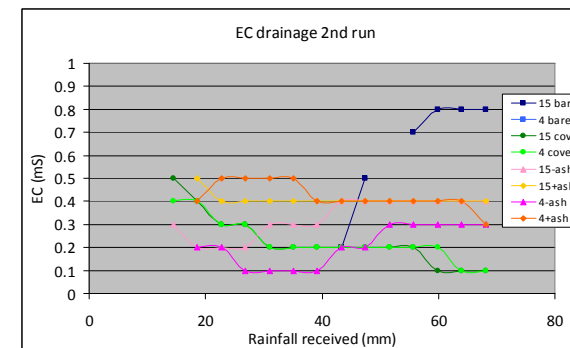
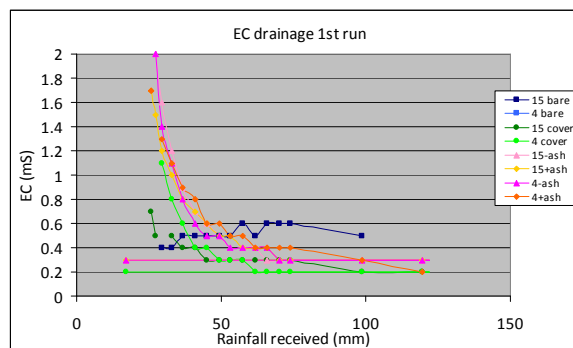


Figure 25 Patterns of EC of drainage water in 1st and 2nd rainfall run

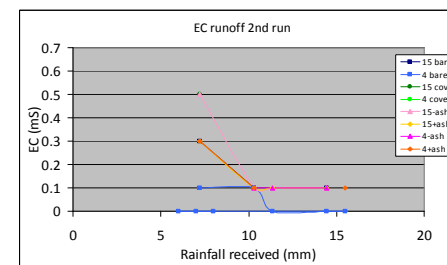
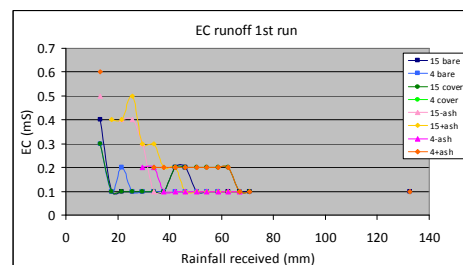


Figure 26 Patterns of EC of runoff water in 1st and 2nd rainfall run

In the second rainfall run the erosion situation is rather different as also the runoff and infiltration patterns are behaving differently compared to the first rainfall run. The first phase of soil loss starts earlier for all treatments, all except one within the 20 mm cum. rain (Figure 24). As is not seen in the first rainfall run at that stage, where the soil loss rates kept rising, after approximately 30 mm a equilibrium is established for all treatments.

The soil loss rates for this run are to be divided in three groups:

- high soil loss rates on the bare control treatments, which has increased compared to first run. Maximum rates that are recorded are 6.9 g mm^{-1} of rain for *4 bare*.
- medium soil loss rates between 2.0 and 2.5 g mm^{-1} for all burned treatments, with no specific difference between the treatments with and without ash cover. Because of that, it is especially an increase in soil wash of the *+ash* cases, as it stayed below 0.6 g mm^{-1} of rain in the first run (Figure 23).
- Zero soil loss for the trays with complete soil cover, as was also the case in run 1. The needles are not washed away and are able to prevent soil erosion during the whole simulated rainy season.

Sediment yield is not (yet) analyzed for composition, so we don't know how much ash and other organic material is washed away or remained on the soil surfaces. Information on the pre-rain and post-rain surface cover is however available in classified feature maps (Appendix IV; Table 8). The fraction of exposed soil is increased in all cases with $>60\%$, especially on *15+ash* this is dramatic, because all ash is washed away or infiltrated in the top soil. *4+ash* lacks a map of the pre-rain conditions, but a difference in the amount of soil with dispersed ash can be observed between the pictures taken after run 1 and after run 2. The ash that remained on the organic material by the 1st run is removed by run 2 and mixing with all remaining exposed soil surface. The classification of burned soil was somewhat problematic because it is chromatically not so different from unburned soil and burned organic material. Yet, a decrease of surface area of blackened affected soil is observable for the *-ash* treatments, while for the *+ash* treatments this is not the case. As the sediment yield of *-ash* is bigger than of *+ash* during the first run, the burned soil may be the main constituent of the sediment, besides ash.

Table 9 Fraction cover features on burned treatments before 1st and 2nd rainfall run (ArcGIS Spatial Analyst, Appendix IV)

TREATMENT		4-ASH		15-ASH		4+ASH		15+ASH	
Surface feature	map color	1st	2nd	1st	2nd	1st ^a	2nd ^b	1st	2nd ^b
soil (not/little affected)	beige	33	67	24	40	48		7	39
burned soil	brown	44	19	62	35			29	33
burned organic	green	7	11	12	14	34	41		28
ash	gray	6		1				63	
charcoal	black	10	3						
soil + ash	brown					18	59		
crack	black				10				

^a the first photo of 4+ash is made **after** the first rainfall simulation

^b the photos used for these classified feature maps are made **after** the 2nd rainfall run

Electrical conductivity

The electrical conductivity (EC) of the drainage and runoff water was measured for all 8 treatments, during both rainfall runs. The drainage of the burned treatments starts with very high salt levels ($1.7 - 2 \text{ mS cm}^{-1}$) but drops very rapidly to levels of $0.2 - 0.6 \text{ mS cm}^{-1}$ which is continued in the second run (Figure 25). The covered treatments start with a lower level (1.1 mS cm^{-1} for *4 cover* and 0.7 mS cm^{-1} for *15 cover*) but decrease with the same speed to a level of 0.2 mS cm^{-1} . In the second run they start with a higher EC value (0.5 mS cm^{-1}) but reach after 30 mm the previous level.

For the bare treatments the story is different. For *4 bare* of run 1 no EC_{drainage} is measured and during run 2 no drainage water is collected, so we depend on the data of *15 bare*. They show the

lowest initial EC value of all with 0.4 mS cm^{-1} . During the first run it remains around the level of 0.5-0.6. At the second run however, another mechanism is operational as EC increases from a level of 0.2 to 0.8 mS cm^{-1} , which is twice as high as the final $\text{EC}_{\text{drainage}}$ level of the other treatments. Because the drainage starts very late, at 43 mm, not many data points are available, but it is clear that the final $\text{EC}_{\text{drainage}}$ level is highest.

The EC pattern of the runoff is less fluctuating and levels decrease over time in both runs (Figure 26). There is no data of 4 cover because no runoff is generated. For the other runs no major difference is observed in initial EC level. After 35 mm (~1h) they all reached a point in stability at an EC-level of $0.1\text{-}0.2 \text{ mS cm}^{-1}$. In the second run the pattern has not changed, but rather quickened, because it takes only 10 mm of received rainfall to get a stable $\text{EC}_{\text{runoff}}$. This takes place, while the runoff volumes and sediment yield is still increasing after 10 mm.

5.2.5 Saturated hydraulic conductivity

Especially after the first rainfall run it was not possible to measure K_{sat} in many places, because the cover with organic material prevented finding large enough places for the MDI. After the second run (MDI2) more measurements were possible which also were more consistent (Table 10).

The hydraulic conductivity is highest on the samples with complete soil cover (50 mm h^{-1}), followed surprisingly by the bare treatments (22 mm h^{-1}). On the burned surfaces the ability of water to infiltrate in the soil smallest, as values range from $1\text{-}16 \text{ mm h}^{-1}$. Reasons for this pattern might be WR and soil sealing in deeper surface layers by the downward moved ash.

Table 10 K_{sat} values (in mm h^{-1}) of first (MDI1) and second (MDI2) measurement with the Mini Disk Infiltrometer on the sample surfaces.

SAMPLE	MDI1			MDI2			AVERAGE		SOIL MOISTURE (%)
	1	2	3	1	2	3	MDI1	MDI2	MDI2
4-ash	7.2			8.4	8.4		7	8	5.0
15-ash				1.2	0.5	16.2 ^a	n.a.	1	6.1
4+ash				3.0	6.6		n.a.	5	14.7
15+ash	0.0 ^a	106.2 ^a		11.4	19.8		n.a.	16	2.3
4 bare	0.4			22.8	33.6	27.6	0	28	4.5
15 bare	17.4	22.8	17.4	14.4	1.8 ^a	17.4	19	16	10.5
4 cover				55.2	64.2	57.6	n.a.	59	17.8
15 cover				49.2	36.6		n.a.	43	38.7 ^b

^a Extreme values, not used for averaging

^b This sample was wet during the MDI experiment

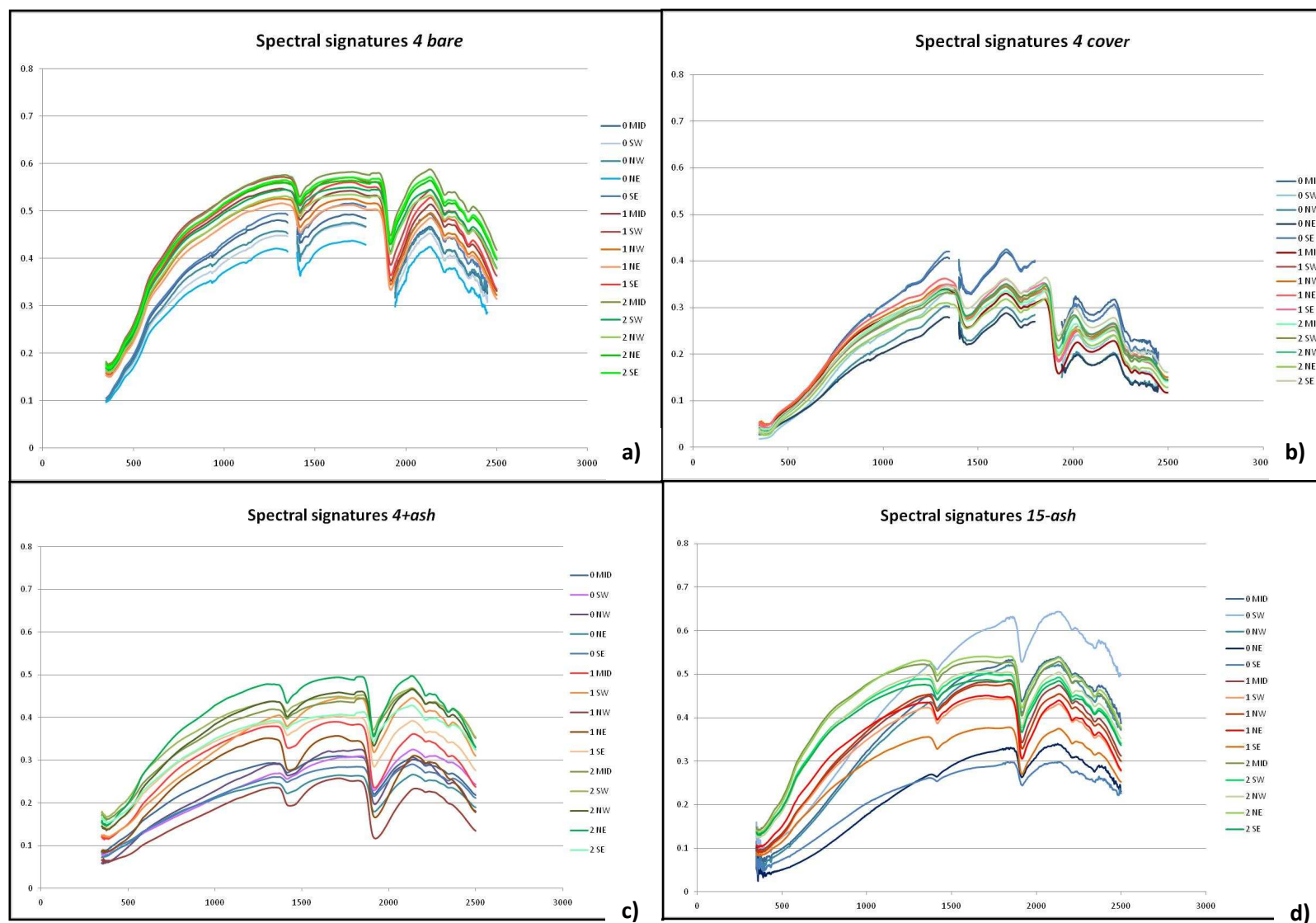


Figure 27 Spectral signatures of averaged point measurements on five sections of the surfaces of samples a) 4bare, b) 4 cover, c) 4+ash, d) 15-ash for 350-2500 nm range. 0 = ASD0, 1 = ASD1, 2 = ASD2, for section positions see Figure 15.

5.2.6 Hyperspectral signatures

At three moments (ASD 0,1,2) during the rainfall simulation series the spectral signature of the surfaces of the samples are recorded and the averaged point measurements of the 5 sections (MID, SW, NW, NE and SE) are displayed (Figure 27). In this report some general remarks about the curves will be made. Detailed analysis of the presence of absorption groups is beyond the scope of this research and will possibly be presented elsewhere.

The soil reflectance spectra in the VIS, NIR and SWIR are characterized by three broad spectral regions at around 1.4, 1.9 and 2.2 μm due to OH^- in water molecules (Ben-Dor *et al.*, 2003).

The signature of the cover sample shows, in contrast to the burned and bare samples, a dip at 2.1 μm (Figure 27). In the typical curve of living vegetation this feature is not found, yet in the spectral signature, of dry

plant material it is occurring, caused by ligno-cellulose absorption (Van der Meer and De Jong, 2002).

Also, a difference between these sample curves is observed at 1.77 μm , where dips due to spectral absorption of bound and unbound water in the needles is taking place (Figure 28).

Another absorption feature is visible at 2330 nm, which is related to carbonate minerals in the soil.

Comparing the -ash and bare spectral curve with +ash, it is observed that the dip is smaller for the latter case as can be caused by measuring less carbonates due to the ash mask.

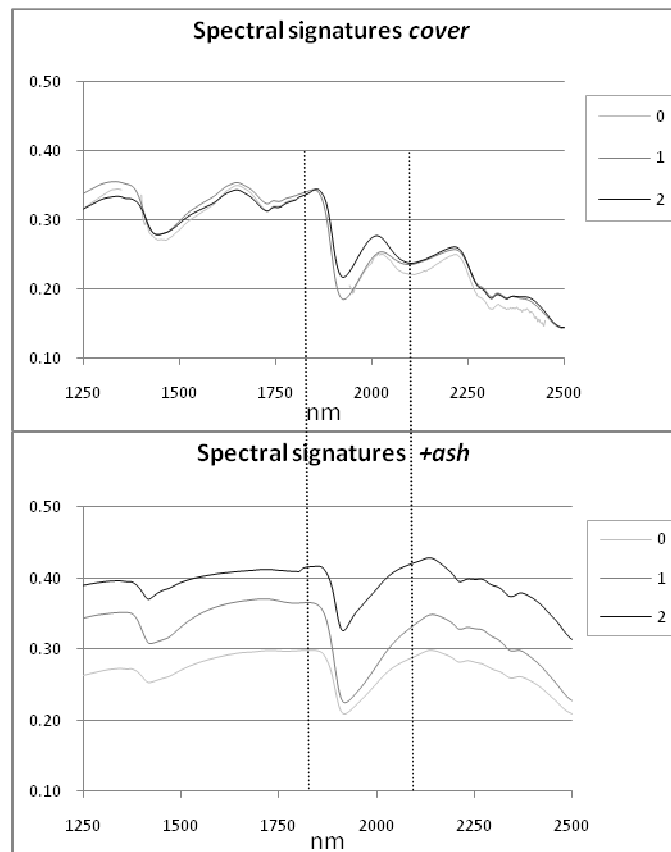


Figure 28 Spectral signature curves of cover and +ash samples for 1.25-2.5 μm range at three moments during the rainfall series. Based on averaged point measurements (#15)

5.2.7 Sections of soil sample volumes

From the photos of the horizons and profiles at the 'upslope' and 'downslope' part of the samples observations can be made about crusting and accumulation of salts in the volume.

The crust of all samples are on average 50 mm, with deviations of 10 mm on other positions of the surface.

In some cases accumulation of carbonates and other salts right below the crust is visible (Figure 29). Aggregates are cemented by the demobilised salts, even in the lower horizons (Figure 30). The charred organic material is transported to the lower soil horizons. The effect of the ash on cementation of the aggregates is from the photos not distinguishable (Figure 30 a,b)



Figure 29 Close-up of crust of bare sample, with accumulated salts (white spots) at bottom.



Figure 30 Close-ups of cemented aggregates and organic material in lower horizon of a) +ash, b) –ash.

Further analysis in terms of classification and determination of the minerals, aggregate structure and ash accumulation is not executed in this experiment. Some more photos are presented in Appendix V.

6. Discussion

6.1 EROSION PARAMETERS

The soil can often be observed as a black box: the type and magnitude of external factors determine its response, visualized in effects on field (micro)morphology, plant development and erosion features. Heating and water affect the soil in such a way that physical change is involved. This research showed on a micro-scale clear differences in water repellency, surface cover changes and hydrological responses when it is subject to a fire and when the ash is removed or maintained. Certini (2005) lists a whole range of soil properties that can be modified or intensified by a wildfire. In the following sections some parameters are selected, which affect erodibility and hydrological responses and are treated in this experimental study.

6.1.1 Vegetation

An important change caused by forest fires is the severe reduction of vegetation cover. It is stated that still 30% of vegetative cover can protect the soil against water erosion (Wittenberg *et al.*, 2007). Short after the fire the risk for soil erosion on slopes is highest because the vegetation recovery does not reach that threshold value. In the study on erosion on Mount Carmel it was found that sediment yields on burned plots in a short-term period after the wildfire reached values which were 100-500 times as high as on the vegetated plots (Inbar *et al.*, 1997). This however decreased rapidly in the following seasons, with runoff decreasing by one order of magnitude and sediment yield by two orders (Inbar *et al.*, 1998). To a large extent this has to do with vegetation recovery in the area. In the first rainy season Inbar *et al.* (1998) recorded re-established vegetation cover of 10-30% of the area, which is greater than our measurements of 1-8 % on the plots where slope process have removed the ash. It is found in the current research that vegetation does not re-establish within 6 months after the fire when the ash layer is still present, which might be due to little light interception of the sprouts under the thick mantle of ash.

The recovery rate of vegetation depends on the angle of the slope facing the sun, rainfall and tree species. Especially pines are rapidly recovering (Inbar *et al.*, 1997) as they re-establish from seed banks in the soil, if not destroyed by the fire. The same is the case for shrubs and grasses, as they re-emerge from underground roots.

The pre-fire vegetation density and soil conditions and corresponding natural runoff can be obtained within several years. (Wittenberg *et al.*, 2007) found the Mediterranean ecological system to be quite resilient, showing a quick response, at least in terms of return to previous states of erosion rates and vegetation cover. On mount Carmel it took a period of 5-10 years for complete recovery of the burned areas and the natural or 'baseflow' sediment amount (Inbar *et al.*, 1998). Cerdà and Doerr (2005) however stated by means of their long-term study of the impact of a Mediterranean fire that the development of soil hydrophobicity can counter some of the effects of vegetation recovery for the amount of overland flow. Compared to shrubs and herbs, pines showed the weakest reduction in overland flow under wet conditions and yet an increase under dry conditions closely related to the fastest increase in soil water repellency due to the hydrophobic nature of pine exudates (Cerdà and Doerr, 2005).

6.1.2 Soil physics and hydrology

Physical change

Fire causes a loss of SOM in the topsoil due to the combustion process. With intensive fires the forest floor as well as the organic soil layer burns, reducing the levels of major plant nutrients (Kutiel and Naveh, 1987). Organic matter and more specifically organic carbon is an important parameter in the erodibility of soils, as it increases aggregate stability by its clay-bonding characteristics. A reduction in SOM therefore can lead to decreased soil resistance against erosive forces (Johansen *et al.*, 2001). Because of the break-down of aggregates and addition clogging of the remaining pores with ash or freed clays, the bulk density of the soil increases (Certini, 2005). This reduces the water holding capacity of the soil, causing lower infiltration capacity and saturated hydraulic conductivity.

K_{sat} values of the experimental soil surfaces after 160 mm of rain is for the burned samples on average $9 (\pm 5)$, for bare 20 and cover 50 mm h^{-1} (Table 10). This is somewhat low when compared with field conditions where K_{sat} is $16 \text{ mm h}^{-1} (\pm 7)$ for the burned plots (Table 6). Besides, the K_{sat} value of the control plot does not reach the high level of the experimental sample with complete soil cover. When comparing the K_{sat} values of MDI2 with the final infiltration rate of run 2, it is striking that in most cases (burned and control) the first is more than 1.5 times as high as the latter. This adds to the suggestion that the point measurement of the MDI is not representative for the surrounding soil surface. The seepage of water is too much affected by macropores, local water repellency, cracks and so on.

Hydrological change

When a heavy Mediterranean autumn rainstorm attacks the recently burned soil, the decreased infiltration capacity, water repellent layer and crust increase the runoff, causing erosion and a higher mudflow risk, especially in an area of steep slopes (Ferreira *et al.*, 2008; Llovet *et al.*, 2009).

These effects are tested in a series of rainfall simulation, with a drying period in between to simulate a wet season fraction.

The hydrological conditions where in run 1 not in equilibrium on the burned samples, as the drainage rates were declining and the runoff rates were decreasing till the termination of the simulation. Because of the kinetic energy of the raindrops the aggregates break down, the smaller particles fill the pores and seal off the soil surface. In run 1 it is still developing, while in run 2 it is a key factor for the runoff pattern. For two treatments it might still be under construction as the drainage rate of *15+ash* and *15-ash* in run 2 is dropping over time. This might also have something to do with the fact that the soil volumes were not completely dried up by the drying period following run 1. Especially the control treatment with full surface cover might have been slow in the drying process.

The sudden drop in infiltration and jump in runoff of *4-ash* is striking. This observation is not made in similar research about rainfall simulation on post-fire soils (e.g. Doerr *et al.*, 2005; Rulli *et al.*, 2006; Johansen *et al.*, 2001; Larsen *et al.*, 2009). The water repellency that is detected on that surface is not very widely present and only slightly – moderate in level (Table 7). But as there are still ash and charcoal/ burned organic pieces present after the 1st run (Appendix IV) they might have been broken down suddenly, clogging the underlying pores, inducing sealing and hampering infiltration at a higher rate than was the case on the other treatments. But the latter remains a mechanism to be clarified.

Focusing a little more on the erosion patterns, it is remarkable that the final runoff rate of the bare treatments is decreased with 9 (*4 bare*) and 15 (*15 bare*) % between the 1st and 2nd run, while the average soil loss has increased with 54 (*4 bare*) and 68 (*15 bare*) %. This means that the

sediment runoff ratio has increased, even when there is a crust on the surface, which enhances soil erodibility. A reason could be the absence of clay-minerals which are washed off in the first run of percolated downwards. This latter was observed at the bottom of the crust where small particles, among others carbonates, were presented and sometimes cemented (Figure 29). The absence of these particles with binding characteristics could cause the possibility for other materials to go into suspension in the water.

Soil chemical changes

The changes in the EC levels of the drainage are most apparent in run 1, as the positions of the surface and soil components are changed by the percolating rainwater. The rainwater itself has zero electrical conductivity, but as it flows through the soil volume several elements are dissolved in it. The decrease in EC can be caused by washing out of the salts and potassium but may also be caused by the binding of cations and clay minerals by organic matter that is moving downward by the percolating rainwater. When one compares the curves of the bare treatment with the treatments where initially organic matter was present on the surface (burned and control with cover), it strikes that the one is increasing/stabilizing while the others are declining over time. Therefore one can state that the organic material is actually moving downward, absorbing salts. The difference in EC between the burned and cover treatment can be due to the amount of organic material available, as a large part of the OM on the burned plots runs off instead of infiltrates.

The mechanism that plays a role in the increase of EC of 4 bare can be explained in several ways also: (1) the forest soil contains SOM which might have been washed out in the previous run and is not available anymore to absorb salts. This phenomenon is reality for all treatments but is masked by the continuous provision of OM from the surface. Rather it is explained by (2) the fact that the soil volume was not completely dried out and that the crust provided a slow infiltration of the water whereby the salts have a lot of time to dissolve in the water before they are drained out.

6.1.3 Ash cover

The ash layer remaining after the simulated fire was much thinner (Figure 29) than the ash layer observed in the field (Figure 4). Hydrological responses, especially in runoff rates in the first stage, which are observed in the rainfall simulation can however be used to estimate field processes. As treatments in which the ash was removed were included, impacts of the ash could be assessed. A important feature of the ash layer is the protection against the energy of raindrops on the soil surface, inducing entrainment of sediment and crust-formation.

The difference in the speed of the development of a crust comparing the bare and the burned treatments is easy to distinguish from the hydrographs. Next to the ash, non-mineral components on the surface and fire-related physiological parameters like WR play a role. Larsen *et al.* (2009) did an extensive research which was fairly similar in objectives and methodology to our study. They also distinguished different ash treatments (bare, low and high) and simulated rainfall on lab boxes with similar size, although with ash that was taken straight from a burned forest (Figure 31). Our results are in line with theirs, as an increase in ash thickness decreases the rate at which runoff increases in time. Our hydrographs of runoff 1 (Figure 17) show the same relative difference as Figure 30. In the second run this pattern is gone due to infiltration or washing off of all ash, as also on the +ash treatment the thickness was not as large as in the research of Larsen *et al.* (2009) where low-ash was ~ 5 mm and high-ash was 12 mm. Cerdà and Doerr (2008) measured the effect of ash and needle cover of a Mediterranean forest and shrubland soil after a wildfire and they concluded that ash has the ability to store large amounts of water, before runoff is initiated. The porosity of ash enables the volume of water that can be stored to be almost equal to the thickness of the layer (Cerdà and Doerr, 2008). Although the

storage of water in run 1 of our experiment is also in the deeper soil layers (as drainage is earlier than runoff), ponding of the water in the ash layer happens and reduces runoff in the later period (Figure 21).

In the first run the soil is protected against the impact of raindrops by the ash cover, like the needles in the control cover treatments have protected the soil completely which is why there exists barely any runoff and no soil loss there.

On the subcanopy field plots the typical ash layer with crust was not washed off in the first 6 months after the fire. The intercanopy plots however, did not have much protective ash left after the rainy season. Apart from the resprouting vegetation, the occurrence of rills showed slope processes in these regions, partly caused by the absence of ash.

The absence of a real ash-crust-layer on the intercanopy plots caused difficulties for classification of surface features. A distinction between soil that is mixed with charred organic material and unaffected soil that is covered with burned material from upslope is hard to make. So the area classified as 'charred organic' and 'soil' might have received sediments from upslope which are deposited there, causing part of the changes in the surface characteristics between 4 and 6 months after the fire.

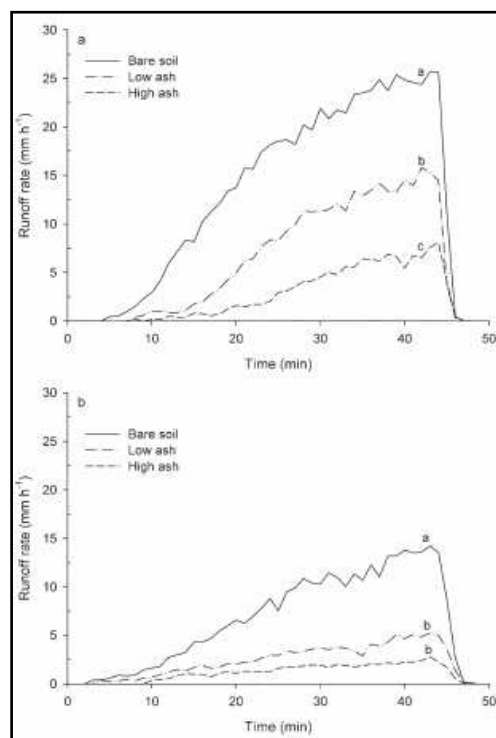


Figure 31 Mean runoff rate over time for the bare-soil, low-ash and high-ash treatments for (a) granitic soil and (b) the micaceous soil. Final runoff rates from treatment with different letters are significantly different at $P < 0.05$ (taken from Larsen *et al.*, 2009)

6.1.4 Water repellency

During our fire simulation experiment temperatures of +280 °C were recorded. According Doerr *et al.* (2005) it is generally agreed that water repellency declines rapidly for wildfires in the high temperature ranges for $T > 250$ °C. They placed sieved samples of naturally water repellent soils (Chernozem, Cambisol, Arenosol and Anthrosol) for fixed times in a muffle furnace at temperatures of 50, (...), 250 and 300 °C. From the research it was concluded that water repellency, which was tested with the Critical Surface Tension test (Letey *et al.*, 2003), was increased in $20 < T < 200$ °C, reduced in the range $200 < T < 300$ °C and would be eliminated at 300 °C when the heating time would be long enough (Doerr *et al.*, 2005).

However the different objectives, soil characteristics and burning method of the current research, it shows results which do not completely agree with the findings of Doerr *et al.* (2005). Both 4-ash and 15-ash are burned with 280 resp. 300 °C, but presence of water repellency after the burn and even after the first rain is detected. Comparing the tests of the +ash cases which are executed after the 2nd run, it is however in line with the findings of mentioned research that treatment 4+ash with T in the most optimal range (170 °C) also has maintained the highest levels of water repellency.

Robichaud and Hungerford (2000) executed laboratory burning experiments to examine water repellency. They used samples with different moisture levels and three heating levels. They ignited the forest floor of the cores (diameter 305 mm) with a radiant propane heater, like we did at first. It is reported that the floor generally burned for several hours, which is very different

from our experiment. The water repellency, which is tested with WDPT, is reported to be highest for the low heat treatment of $100 < T < 150$ °C, while only slightly for the moderate heat treatment of $250 < T < 300$ °C burned under dry moisture conditions. This result does not agree with the recorded water repellency levels in the field, where the forest has suffered from a high intensity fire in which temperatures can reach easily 600 °C at the surface.

Hydrological responses of WR

The temperatures of the simulated fire had high enough temperatures (175 – 280 °C) to change or intensify the degree of water repellency at the soil surface. But because different mechanisms are playing a part in the rainfall experiment (sink dynamics, crusting and others), it is difficult to distinguish the ruling factors at particular moments. The drainage and runoff hydrographs of the samples show an steady development for the whole simulation duration, but I like to elaborate on some small drops and rises in the curves.

In the runoff curves of *4-ash* and *15-ash* of run 1 two things are standing out. After 54 mm of rain the runoff rate of *4-ash* is suddenly declining and establishes a more horizontal pathway of increase in runoff rate, from 1.02 to 0.14 mm h⁻¹ per mm accumulated rain. For *15-ash* this happens a little later, at 75 mm of rain. This same pattern is also visible at the curve of *15+ash* at 70 mm (Figure 21).

These drops of >1 mm h⁻¹ in runoff can be caused by reading errors, but in two of these three cases a sudden and temporary ‘freeze’ of drainage level is acquired at the same time (Figure 19). At 54 mm the drainage curve of *4-ash* is horizontal, and the same counts for *15-ash* at 73 mm. Taking into account the little delay, a reason for this change in the almost linear curves might be a break-down of the subsurface water repellent layer causing a momentary freeze in drainage decline, which causes for a short time more drainage and no further increase in runoff. Another factor might be the breakdown of the present surface WR, whereby the sinks in the vicinity of these hydrophobic areas loose their function and the runoff water has more area to infiltrate. After several mm of rain a new equilibrium is established where the crust formation plays still a key role and masks other hydrological relationships.

Spatial variation in WR

When WR is measured in nearby grid cells, hydrophobic soil patches can be distinguished. In our experiment, their size is not large, each having a size of 10 (half a grid cell) to 25 cm². The most extensive patches with moderate–strong WR (50 cm²) were found on *4-ash* and *15+ash* surfaces (Appendix II). As in part 6.1.2 was mentioned, the jumps in infiltration of *4-ash* might be due to the ponding on these patches. Sample *15+ash* has also the largest total patch area with 175 cm² which makes up 12% of the total surface.

The preferential flows are modeled using the data on water repellency of the surface, but other surface features like sediment catching and soil roughness are not taken into account. As the single patches measure around 3 % of the total surface the effect of this source area is small. The effect of all patches together (max 12%) can be taking into account, but one should notice that the patches are often not connected. Accumulation of water and an actual run from source to sink is therefore not very realistic in this experiment.

In the field, in both sub- and surface layers extreme WR is observed. In 1.5 months the wettable and slightly hydrophobic area has increased, but in the subsurface area the extreme values are not diminished (Figure 17a,c). Differences related to distance from the tree are not clearly discerned from the data. It is observed that further from the tree (1m) higher WR occurs at the surface and closer to the tree (0.5m) this is present in the subsurface. It is assumed that most needles are present near the tree trunk and that fire is most severe. The hydrophobic compounds could therefore be move further down, compared to locations less under the canopy.

The measurements that are executed 5 months later show completely different results (Figure 17d): 95% of surface area is extremely water repellent and also the subsurface area with high WR

values increased. The analysis is based on less point measurements (120), than the earlier tests 240 and 287 for 0.5 resp. 1.5 month after the fire). Also, because the test is done by another team than the earlier tests, another way of selecting subsurface layer and removing ash from the surface could have been applied, causing inconsistency in the series of WR data.

Testing WR

Apart from the currently Water Drop Penetration Time (WDPT) test, characterizing physical water repellency can be done by many other methods, for example by wetting coefficients and surface roughness (DeBano, 2003). Identifying hydrophobicity of small patches in the field and to assess the vertical distribution can be done by the Critical Surface Tension (CST) test. WDPT provides information on the stability of the repellency, while other methods (ninety degree surface tension e.g.) indicate the degree of water repellency (Letey *et al.*, 2003)

Moderate water repellency levels are found on the sample surfaces, but as this feature is not checked on the subsurface after the burn and the first rainfall, it is not known if water repellency was present on other places in the soil volume. Woods *et al.* (2007) decided not to measure subsurface water repellency when the surface was hydrophilic, because preliminary measurement in the 0-5 cm depth interval clearly showed that the strongest WR was at the surface. This is also consistent with other studies with moderate fire severities (Huffman *et al.*, 2001), where WR decreased with depth.

However, if WR is existing in subsurface layers, it is described in literature that they can block further infiltration of percolated water. During storms this may cause rapid saturation of the upper wettable layer, which on sloping terrain may be removed by overland flow, implicating damage to the environmental conditions (Doerr *et al.*, 2006).

6.2 EXPERIMENTAL SET-UP

The reliability of the experiment can be liable to errors due to several features of the experimental set-up.

The rainfall intensity of 33 mm h⁻¹ of the rainfall simulator is chosen to be resembling with intensities of natural rain events in the Mediterranean climate. Because we wanted to know exactly how much water comes in the system, as we know how much comes out in terms of runoff and throughflow, the precipitation had to be stable. One must keep in mind that in natural Mediterranean rain events this barely happens, as the rain comes in intensive storms of short duration. From this research it was however found that under bare, low-ash and high-ash conditions erosion can reach high values under such rainfall intensities. Though this is not fitting for this micro-scale research, when scaling up the volumes of soil loss for *ash* surfaces to a hectare it gives under this rain intensity an hourly loss of 0.2 ton and in a later stage of the season 0.8 ton. And when the field would be disturbed after the fire the field would lose at the start of the rainy season about 0.4 t ha⁻¹ hr⁻¹.

During the first run the soil loss caused a lowering of the soil level, which was initially several mm above the top of the through. During the second level the sediments might have partly been accumulated at the lower end of the box and have not transported through the outlet. The soil loss in run 2 might accordingly be in reality some higher.

The techniques and methodologies in the field are also subject to uncertainties. The technique of photographing the plots is a point of discussion, as the plot maps are not square, differing in shape for both recording dates and have different illumination (one day was cloudy weather, the other day sunshine). In one of the maps (plot 3, +6 month) shadows are observable, which are caused by trees on the steep terrain.

The classification result is not checked for omission and commission errors in a post-classification procedure. Therefore the validity of the maps is negotiable.

The hyperspectral signatures of the sections are not in all ASD test cases representative for the whole sample surface, as the reflectance values of the sections of *cover* and *-ash* differ for one test (ASD0) more than the tests differ from each other (Figure 27b,d). For one ash-less treatment (*15-ash*), spatially varying burn severities could have produced differences in removal or breaking-down of aggregates and minerals, resulting in contrasting shapes of the section signatures. The different curves of ASD0 of *4 cover* could be based on initial moisture content variation of the applied needles, due to the moisture gradients in the natural needle layer which was taken from a forest and used for the experiment.

Ignoring mentioned differences of ASD0, the albedo of all treatments increases over time. As moisture absorbs radiation over the whole spectrum, a higher reflection indicates drier sample surfaces. However, as the surfaces were oven-dry at ASD0, the differences with ASD1 and ASD2 could also be caused by the observed crusting, as this process smoothes the surface and increases albedo, too.

In general, it can be seen that the spectral signatures of *4 cover* and to a lesser extent of *4+ash* have a lower albedo, thanks to organic matter which reduces the overall reflectivity of the soil (Van der Meer and De Jong, 2002).

7. Conclusion

Fire and rainfall simulation experiments were executed to evaluate the short-term effects of a fire on the hydrological and erosion-related parameters of a forest soil. The moderate fire severity altered the soil surfaces to the degree that drainage decreased and runoff increased. Water repellency of the surfaces was induced and remained present after >140 mm of simulated rain. The runoff and soil loss values during the first 70 mm of rain were lower than under bare conditions, indicating the protecting function of the ash layer and the infiltration-improving characteristics of OM and ash. With a further increase in precipitation, the differences between bare control and burned samples cease to exist.

Simulations are done on undisturbed burned soil samples (*+ash*), burned samples where the ash is removed (*-ash*) and control soil samples with (*cover*) and without (*bare*) a litter layer. The manually simulated fire combusted all litter cover and induced water repellency on all surfaces. Strong WR-levels (61-300 s.) are recorded 24h after the burn on parts of the surface of *15-ash*; other samples showed slight-moderate levels. Two rainfall simulations (140 mm cum. rain) decreased the hydrophobicity level in most cases, although still WR is present on the surface. For reasons of preventing disturbance, subsurface measurement of WR are not executed.

The experiment was executed for two aggregate sizes (4 and 15 mm), but as the initial conditions in terms of fire intensity, fuel load and ash cover were different for each sample, a valid assessment of the impact on aggregate size on hydrological behavior and WR can not be made.

On the control samples equilibrium drainage rates of 33 mm h⁻¹ for *cover* and 0-1.6 mm h⁻¹ for *bare* are recorded. The infiltration rates for the burned samples are for the first run between mentioned values, with *-ash* below *+ash*, but in the second run the drainage values are close to the small drainage rate of the *bare* treatments (1-6 mm h⁻¹). For the runoff rates this is inversely comparable. The control treatments have erosion rates of 0-1 mm h⁻¹ for *cover* and 25-28 mm h⁻¹ for *bare*, and the burned erosion rates are between these limits. No soil loss is detected on the samples with complete needle cover, while the sediment yields for the bare samples reached 6 g mm⁻¹ of rain (13 t ha⁻¹ h⁻¹). The burned samples reach soil loss values of 0.5 - 2.5 g mm⁻¹ (*-ash* resp. *+ash*). In the second run the erosion and soil loss rates of burned and *bare* surfaces are comparable, indicating diminishing ash protection and crusting as a large erodibility factor.

Variations in the drainage and runoff hydrographs are for the burned samples larger than for the control treatments. During the first rains (60 mm), the drainage in the ash-covered samples was twice as high as in the samples where the ash was removed. This ash cover protects the surface from the impacts of raindrops and stores water which is not available for runoff. However, through rain ash washes off or fills pores between the soil aggregates, leaving after about 60 mm a non-protected burned soil. After the first run most ash and organic material was washed off and saturated hydraulic conductivity was low, indicating crust formation.

Sudden changes in runoff and drainage on the burned samples, indicated the momentarily importance of factors as water repellency. Eventually, soil crusting is the determining factor for the hydrological responses.

Measurements on the burned field of Peér'am catchment show that during the rainy season the vegetation in intercanopy conditions recovers faster than in the subcanopy positions, although in general it is slow because of the northeast facing slope. On the other hand, the thicker ash layer under the (burned down) trees protects the soil against the drops, as in the intercanopy positions small rills were visible and down the slope sediments consisting of organic and mineral soil particles were visible.

The water repellency measurements around the trees on three moments in time (0.5, 1.5 and 6.5 months after the fire) shows that subsurface WR (-5 cm s.l.) is declining but that surface (below ash) maintains a strong-severe WR level.

7.1 IMPLICATIONS

The outcomes of this study may contribute to designing best management practices after a fire. As it is shown that runoff is increased when the ash layer is disturbed and partly removed, it may be wise to refrain from treading the burned area before the first rains have come.

As is also shown in other research, hydrophobicity of surface and subsurface layers fades not in a short-term period. Slight-moderate levels at the surface are not removed by >140 mm of rain (lab) and severe levels at the (sub)surface not by >600 mm of rain (field). If the water repellency is present in a whole layer and at a high enough level and all protective cover is burned, this may pose serious risks of slope wash. Therefore it is advised to install, after a fire of high intensity at a steep slope, sediment catchers at intervals along the slope to mitigate off-side effects of slope wash.

Next, the results in the field on the subcanopy plots show that a thick ash layer impedes the fast establishing of new vegetation which can decrease the erodibility of the hillslope. In order to improve regeneration of vegetation raking of the ash layer may be an option to create similar circumstances as the intercanopy plots where resprouting was visible 6 months after the fire. It must be added that this should not be done before the rainy season, as the soil needs especially then the protection of the ash layer against the raindrops.

7.2 FURTHER RESEARCH

This research has produced interesting data on erodibility of forest soils impacted by a fire, and is mainly confirming other research work in the areas of fire-induced water repellency and rainfall simulation. However, it must be stressed that there are still many gaps to be filled. Firstly, in order to validate the datasets more repetitions of the treatments need to be made. The internal variation of the +ash and -ash cases is yet too big to apply statistical analysis of the results. Recommended is to record detailed fire characteristics (horizontal and vertical temperature gradients in tray, temperature fluxes over time) to know the starting conditions and to be able to relate it to the spatial pattern of water repellency.

Secondly, water repellency should be measured at specific times consistently for all treatments. The test after the burn should be done > 1 day later to equilibrate.

Regarding the experimental design of the treatments more insight of micro field conditions would be gained by adding burned treatments with unburned needles to the rainfall simulation. By this method the relative importance of complete soil cover and water repellency to drainage and runoff can be investigated.

8. References

- Analytical Spectral Devices, Inc. Instrumentation and Accessoires. <http://www.asdi.com/products>. Apr, 2010.
- Ben-Dor, E., Goldshleger, N., Benyamini, Y., Agassi, M. and Blumberg, D.G., 2003. The spectral reflectance properties of soil structural crusts in the 1.2- to 2.5- μ m spectral region. *Soil Science Society of America Journal* 67(1): 289-299.
- Bodner, J., 2007. The Recovery of Northern Israel Through a Forest's Eyes. Jewish National Fund.
- Cerdà, A., Ibáñez, S. Calvo, A. 1997. Design and operation of a small and portable rainfall simulator for rugged terrain. *Soil Technology* 11(2): 163-170.
- Cerdà, A. and Doerr, S.H., 2005. Influence of vegetation recovery on soil hydrology and erodibility following fire: an 11-year investigation. *International Journal of Wildland Fire*, 14(4): 423-437.
- Cerdà, A. and Doerr, S.H., 2008. The effect of ash and needle cover on surface runoff and erosion in the immediate post-fire period. *CATENA*, 74(3): 256-263.
- Certini, G., 2005. Effects of Fire on Properties of Forest Soils: A Review. *Oecologia*, 143(1): 1-10.
- DeBano, L.F., 2000. The role of fire and soil heating on water repellency in wildland environments: a review. *Journal of Hydrology*, 231-232: 195-206.
- DeBano, L.F., 2003. The role of fire and soil heating on water repellency. In: C.J. Ritsema and L.W. Dekker (Editors), *Soil Water Repellency: occurrence, consequences and amelioration*. Elsevier, Wageningen, pp. 193-202.
- Doerr, S.H. *et al.*, 2005. Effects of heating and post-heating equilibration times on soil water repellency. *Australian Journal of Soil Research*, 43(3): 261-267.
- Doerr, S.H. *et al.*, 2006. Effects of differing wildfire severities on soil wettability and implications for hydrological response. *Journal of Hydrology*, 319(1-4): 295-311.
- Doerr, S.H., Shakesby, R.A. and MacDonald, L.H., (in press). Soil Water Repellency: A Key Factor in Post-Fire Erosion? In: A. Cerdà and P. Robichaud (Editors), *Restoration Strategies after Forest Fires*.
- Doerr, S.H., Shakesby, R.A. and MacDonald, L.H., in press. Soil Water Repellency: A Key Factor in Post-Fire Erosion? In: A. Cerdà and P. Robichaud (Editors), *Restoration Strategies after Forest Fires*.
- Doerr, S.H., Shakesby, R.A. and Walsh, R.P.D., 2000. Soil water repellency: its causes, characteristics and hydro-geomorphological significance. *Earth-Science Reviews*, 51(1-4): 33-65.
- Elliot, W.J., Robichaud, P.R. and Pannkuk, C.D., 2001. A Probabilistic Approach To Modeling Erosion for Spatially-Variied Conditions, American Society of Agricultural Engineers Annual International Meeting, Sacramento, California, USA.
- Ferreira, A.J.D., Coelho, C.O.A., Ritsema, C.J., Boulet, A.K. and Keizer, J.J., 2008. Soil and water degradation processes in burned areas: Lessons learned from a nested approach. *CATENA*, 74(3): 273-285.
- Fox, D., Berolo, W., Carrega, P. and Darboux, F., 2006. Mapping erosion risk and selecting sites for simple erosion control measures after a forest fire in Mediterranean France. *Earth Surface Processes and Landforms*, 31(5): 606-621.
- Franzluebbers, A.J., 2002. Water infiltration and soil structure related to organic matter and its stratification with depth. *Soil and Tillage Research*, 66(2): 197-205.
- Ginsberg, P., 2006. Restoring biodiversity to pine afforestations in Israel. *Journal for Nature Conservation*, 14(3-4): 207-216.
- Huffman, E.L., MacDonald, L.H. and Stednick, J.D., 2001. Strength and persistence of fire-induced soil hydrophobicity under ponderosa and lodgepole pine, Colorado Front Range. *Hydrological Processes*, 15(15): 2877-2892.

- Hudson, N.W., 1993. Field measurement of soil erosion and runoff. Chapter 6. Rainfall simulators. FAO Soils Bulletin 68.
- Israel Meteorological Services, 2010. Rainfall observations Har Kenaan (Zefat). www.ims.gov.il, visited Apr, 2010.
- Inbar, M., Tamir, M. and Wittenberg, L., 1998. Runoff and erosion processes after a forest fire in Mount Carmel, a Mediterranean area. *Geomorphology*, 24(1): 17-33.
- Inbar, M., Wittenberg, L. and Tamir, M., 1997. Soil Erosion and Forestry Management After Wildfire in a Mediterranean Woodland, Mt. Carmel, Israel. *International Journal of Wildland Fire*, 7(4): 285-294.
- Johansen, M.P., Hakonson, T.E. and Breshears, D.D., 2001. Post-fire runoff and erosion from rainfall simulation: contrasting forests with shrublands and grasslands. *Hydrological Processes*, 15(15): 2953-2965.
- Keeley, J.E., 2009. Fire intensity, fire severity and burn severity: a brief review and suggested usage. *International Journal of Wildland Fire*, 18(1): 116-126.
- Kemper, W.D. and Rosenau, R.C., 1986. Aggregate stability and size distribution. In: A. Klute (Editor), *Methods of Soil Analysis. Part I. Physical and Mineralogical Methods*. Agronomy Monograph No. 9. American Society of Agronomy, Soil Science Society of America, Madison, WI, pp. 425-442.
- Kukul, S.S. and Sur, H.S., 2004. A simple and portable rainfall simulator for erosion studies. *Agricultural Engineering India*, 85(1): 55-57.
- Kutiel, P. and Naveh, Z., 1987. The effect of fire on nutrients in a pine forest soil. *Plant and Soil*, 104(2): 269-274.
- Larsen, I.J. *et al.*, 2009. Causes of Post-Fire Runoff and Erosion: Water Repellency, Cover, or Soil Sealing? *Soil Sci Soc Am J*, 73(4): 1393-1407.
- Lebron, I., Madsen, M.D., Chandler, D.G., Robinson, D.A., Wendroth, O., Belnap, J., 2007. Ecohydrological controls on soil moisture and hydraulic conductivity within a pinyon-juniper woodland. *Water Resources Research* 43, W08422.
- Lentile, L.B. *et al.*, 2006. Remote sensing techniques to assess active fire characteristics and post-fire effects. *International Journal of Wildland Fire*, 15(3): 319-345.
- Letey, J., Carillo, M.L.K. and Pang, X.P., 2003. Characterizing the degree of repellency. In: C.J. Ritsema and L.W. Dekker (Editors), *Soil Water Repellency: occurrence, consequences and amelioration*. Elsevier, Wageningen, pp. 51-56.
- Lewis, S.A., Robichaud, P.R., Frazier, B.E., Wu, J.Q. and Laes, D.Y.M., 2008. Using hyperspectral imagery to predict post-wildfire soil water repellency. *Geomorphology*, 95(3-4): 192-205.
- Lewis, S.A., Wu, J.Q. and Robichaud, P.R., 2006. Assessing burn severity and comparing soil water repellency, Hayman Fire, Colorado. *Hydrological Processes*, 20(1): 1-16.
- Llovet, J., Ruiz-Valera, M., Josa, R. and Vallejo, V.R., 2009. Soil responses to fire in Mediterranean forest landscapes in relation to the previous stage of land abandonment. *International Journal of Wildland Fire*, 18(2): 222-232.
- Mataix-Solera, J. and Doerr, S.H., 2004. Hydrophobicity and aggregate stability in calcareous topsoils from fire-affected pine forests in southeastern Spain. *Geoderma*, 118(1-2): 77-88.
- Morin, J. and Cluff, C.B., 1980. Runoff calculation on semi-arid watersheds using a rotadisk rainulator. *Water Resources Research* 16(6):1085-1093.
- Neary, D.G., Klopatek, C.C., DeBano, L.F. and Ffolliott, P.F., 1999. Fire effects on belowground sustainability: a review and synthesis. *Forest Ecology and Management*, 122(1-2): 51-71.
- Pausas, J.G. and Vallejo, V.R., 1999. The role of fire in European Mediterranean Ecosystems. In: E. Chuvieco (Editor), *Remote sensing of large wildfires in the European Mediterranean basin*. Springer-Verlag, pp. 3-16.
- Pyne, S.J., Andrews, P.L. and Laven, R.D., 1996. *Introduction to Wildland Fires*. John Wiley & Sons, Inc., New York.
- Robichaud, P.R., 2000. Fire effects on infiltration rates after prescribed fire in Northern Rocky Mountain forests, USA. *Journal of Hydrology*, 231-232: 220-229.
- Robichaud, P.R. and Hungerford, R.D., 2000. Water repellency by laboratory burning of four northern Rocky Mountain forest soils. *Journal of Hydrology*, 231-232: 207-219.







- Rulli, M.C., Bozzi, S., Spada, M., Bocchiola, D. and Rosso, R., 2006. Rainfall simulations on a fire disturbed mediterranean area. *Journal of Hydrology*, 327(3-4): 323-338.
- Tan, K.H., 2005. Soil sampling, preparation, and analysis. 2nd Edition. Taylor & Francis Group, 639 pp.
- Tessler, N., Wittenberg, L., Malkinson, D. and Greenbaum, N., 2008. Fire effects and short-term changes in soil water repellency - Mt. Carmel, Israel. *CATENA* 74: 185-191.
- Úbeda, X. and Mataix-Solera, J., 2008. Fire effects on soil properties: A key issue in forest ecosystems. *CATENA*, 74(3): 175-176.
- Van der Meer, F.D., De Jong, S.M., 2002. Basic Physics of Spectrometry. Remote Sensing and Digital Image Processing. Springer, the Netherlands.
- Wittenberg, L., Malkinson, D., Beerli, O., Halutzy, A. and Tesler, N., 2007. Spatial and temporal patterns of vegetation recovery following sequences of forest fires in a Mediterranean landscape, Mt. Carmel Israel. *CATENA*, 71(1): 76-83.
- Woods, S.W. and Balfour, V.N., 2008. The effect of ash on runoff and erosion after a severe forest wildfire, Montana, USA. *International Journal of Wildland Fire*, 17(5): 535-548.
- Woods, S.W., Birkas, A. and Ahl, R., 2007. Spatial variability of soil hydrophobicity after wildfires in Montana and Colorado. *Geomorphology*, 86(3-4): 465-479.

Appendices

- I. Classified feature maps field
- II. Map overlay of WR grid and picture
- III. Map overlay of Preferential flow and photo
- IV. Classified feature maps laboratory
- V. Close-up photos of features on soil samples

Appendix I. Classified feature maps field plots 1-5

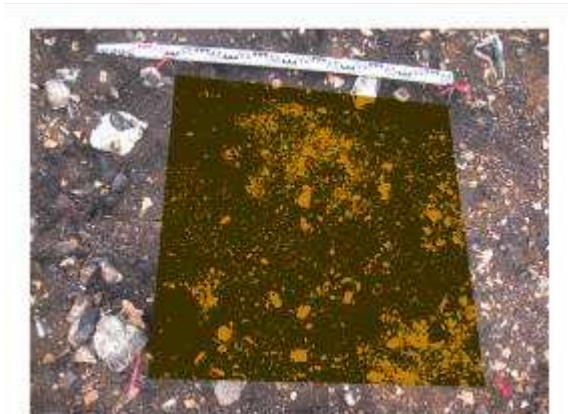
Legend

	black soil
	ash
	burned organic material
	soil
	stones
	living vegetation

Colors can be slightly different on the map

Plot 1

+ 4 month



+ 6 month



Plot 2

+4 month

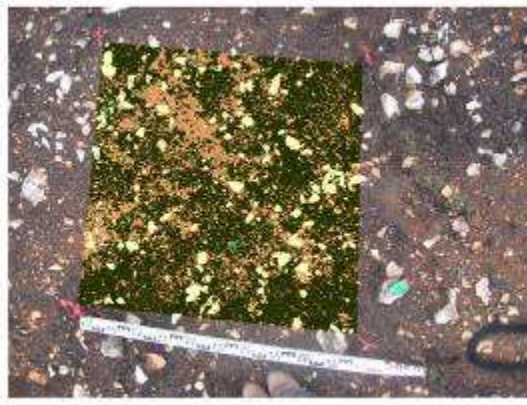


+ 6 month



Plot 3

+4 month

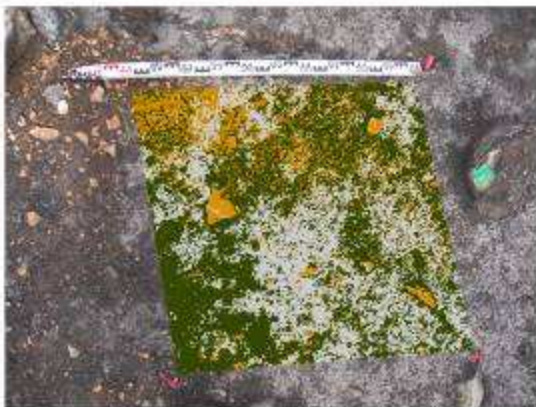


+ 6 month



Plot 4

+ 4 month

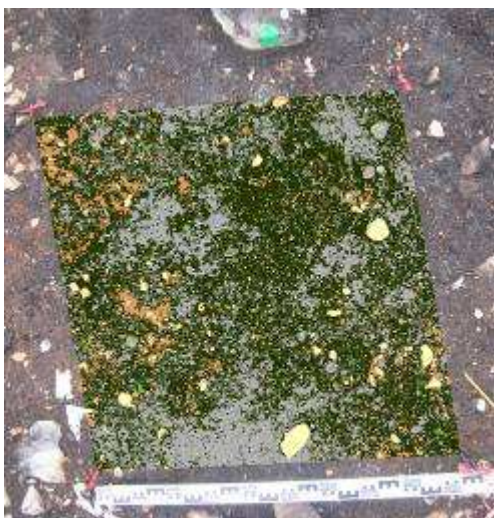


+6 month



Plot 5

+ 4 month



+ 6 month



Appendix II. Map overlay of WR grid and picture

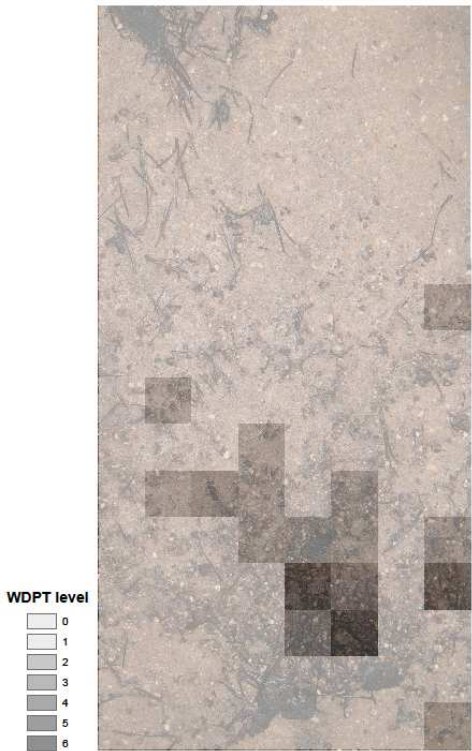
Level 0	= no data
Level 1	= hydrophilic
Level 2 – 8	= hvdrophibic

4-ash

WR 1

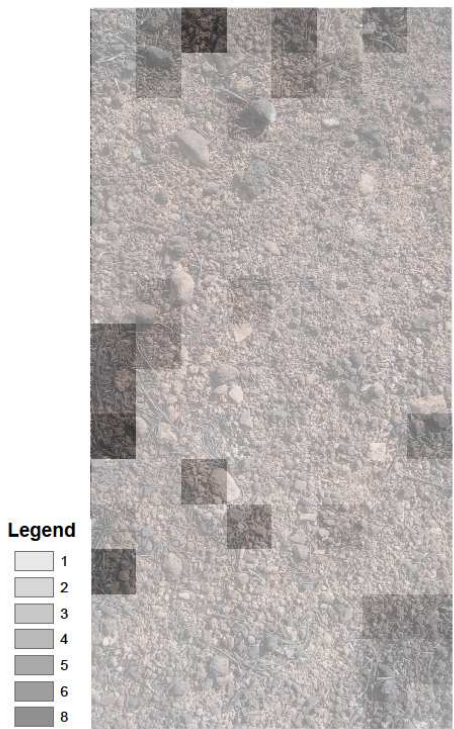


WR 2



15-ash

WR 1

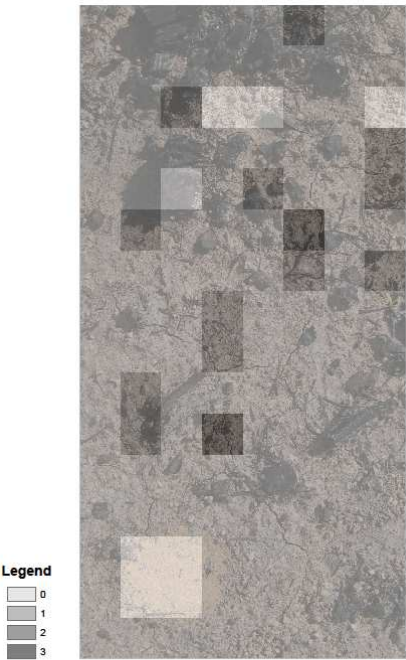


WR 2



4+ash

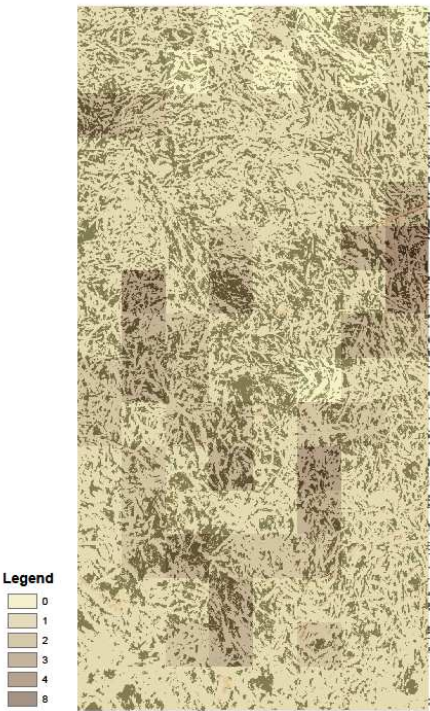
WR 2



Overlay WR grid with photo
4B WR2

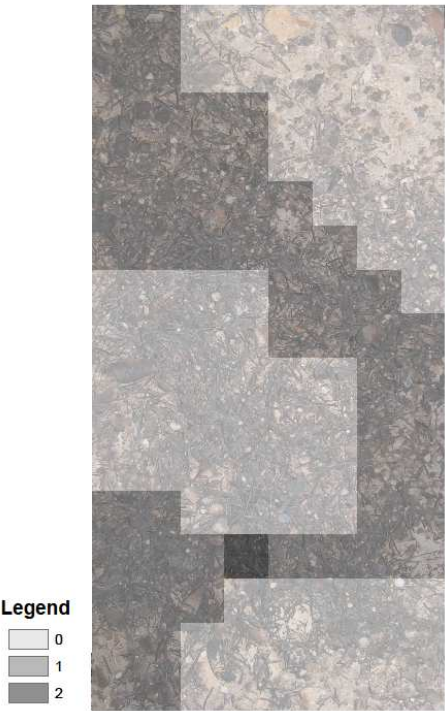
15+ash

WR 1



Overlay WR grid and photo
3C WR1

WR 2



Overlay WR grid and photo
3C WR2

Appendix III. Map overlay of Preferential flow and photo

Legend feature map

Black	charcoal (fields) or cracks (lines)
Gray	ash
Brown	burned exposed soil
Green	burned organic material
Beige	exposed soil, no or little burned

4-ash

Run 1

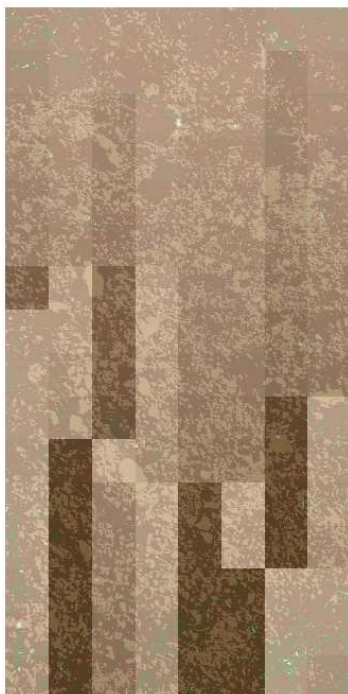


Run 2



15-ash

Run 1



Run 2



4+ash

Run 2



15+ash

Run 1



Run 2



Appendix IV. Classified feature maps laboratory experiment

Legend

- soil (not/little affected)
- burned soil (with ash)
- ash
- charcoal
- burned organic material

Colors can be slightly different on the map

4-ash

before 1



before 2



15-ash

before 1



before 2



after 1



4+ash

after 2



15+ash

before 1



after 2



Appendix V. Close-up photos of features on soil samples



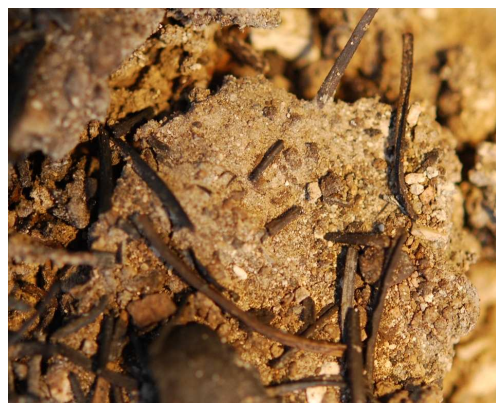
The typical needle cover of *control cover* samples



Crust of *4 bare* sample



Crust of *-ash* sample



Crust of *+ash* sample



Profile from top to bottom of *4 bare*



Features after rainfall
run 1 on *+ash* sample:
cemented aggregate
(top) and ash on
surface (bottom)